UNIVERSIDADE FEDERAL DO PARANÁ

ANNA GABRIELLA TEMPESTA

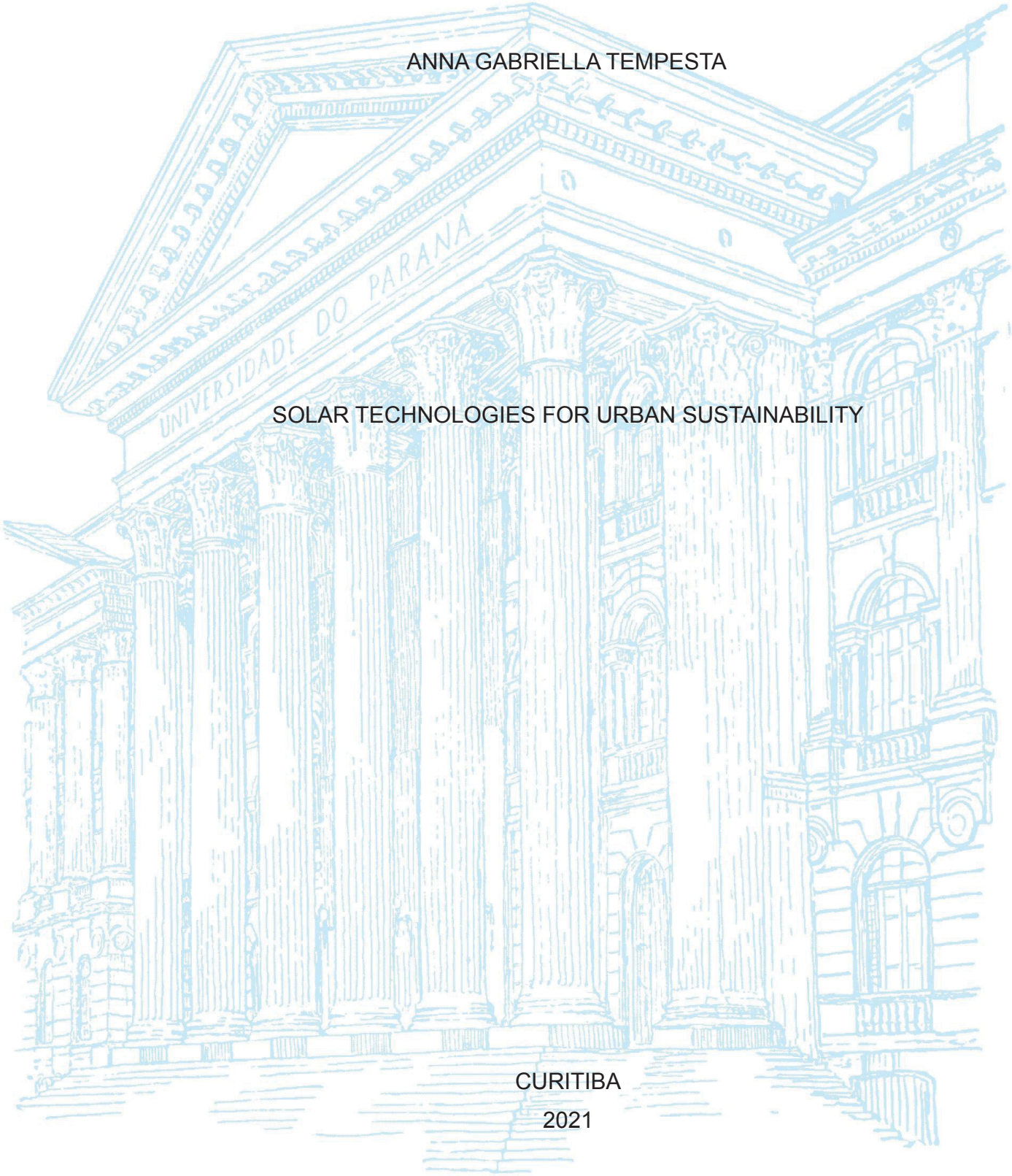

SOLAR TECHNOLOGIES FOR URBAN SUSTAINABILITY

CURITIBA

2021

ANNA GABRIELLA TEMPESTA

SOLAR TECHNOLOGIES FOR URBAN SUSTAINABILITY

Tese apresentada ao curso de Pós-Graduação em Engenharia e Ciências dos Materiais, Setor de Tecnologia, Universidade Federal do Paraná, como requisito parcial à obtenção do título de Doutor em Engenharia e Ciência de Materiais.

Orientadora: Profª. Dra. Lucimara Stolz Roman

CURITIBA

Catalogação na Fonte: Sistema de Bibliotecas, UFPR
Biblioteca de Ciência e Tecnologia

T283s Tempesta, Anna Gabriella
Solar technologies for urban sustainability [recurso eletrônico] / Anna Gabriella Tempesta. – Curitiba, 2021.

Tese - Universidade Federal do Paraná, Setor de Tecnologia, Programa de Pós-Graduação em Engenharia e Ciências dos Materiais, 2021.

Orientador: Lucimara Stolz Roman.

1. Mobiliário urbano. 2. Sustentabilidade. 3. Geração de energia fotovoltaica. I. Universidade Federal do Paraná. II. Roman, Lucimara Stolz. III. Título.

CDD: 621.31244

Bibliotecária: Vanusa Maciel CRB- 9/1928

TERMO DE APROVAÇÃO

Os membros da Banca Examinadora designada pelo Colegiado do Programa de Pós-Graduação em ENGENHARIA E CIÊNCIA DOS MATERIAIS da Universidade Federal do Paraná foram convocados para realizar a arguição da tese de Doutorado de **ANNA GABRIELLA TEMPESTA** intitulada: **SOLAR TECHNOLOGIES FOR URBAN SUSTAINABILITY** , sob orientação da Profa. Dra. LUCIMARA STOLZ ROMAN, que após terem inquirido a aluna e realizada a avaliação do trabalho, são de parecer pela sua aprovação no rito de defesa.

A outorga do título de doutora está sujeita à homologação pelo colegiado, ao atendimento de todas as indicações e correções solicitadas pela banca e ao pleno atendimento das demandas regimentais do Programa de Pós-Graduação.

CURITIBA, 29 de Setembro de 2021.

LUCIMARA STOLZ ROMAN
Presidente da Banca Examinadora

MARCELA MOHALLEM OLIVEIRA
Avaliador Externo (UNIVERSIDADE TECNOLÓGICA FEDERAL DO PARANÁ)

MARLUS KOEHLER
Avaliador Externo (UNIVERSIDADE FEDERAL DO PARANÁ)

MARIA LUIZA ROCCO DUARTE PEREIRA
Avaliador Externo (UNIVERSIDADE FEDERAL DO RIO DE JANEIRO)

ANTONIO FERREIRA DA SILVA
Avaliador Externo (UNIVERSIDADE FEDERAL DA BAHIA)

To my daughter Alicia and to Prof. Susana Reinecke
(in memoriam)

Acknowledgements

I would like to thank my advisor, Prof. Lucimara Stolz Roman, for believing in the project and encouraging me in every step of the way. DiNE is a neat research group and Prof. Lucimara's way of leading helps every group member to reach their best.

Being in this research group is a bless and I would like to thank each of my colleagues for their help and cooperation. Luiz, Fabi, Talitha, Henrique and Kaike you are the best collaborators I could wish for.

Coming back to UFPR after many years was a joyful experience. I take this opportunity to thank the university, specially Prof. Graciela Muniz as she is the one responsible for my coming to UFPR. I also thank the graduate program on Materials Science and Engineering for accepting this project and Maria Neiva Rodrigues Fedechem for the support with the program regulations and deadlines.

I am grateful to the supporters of this project, URBS - specially Olga Mara Prestes. I also thank COPEL, CSEM/Sunew and JSchebly. CNPq also supports the research at DiNE/UFPR, thank you!

Many thanks to the referee panel for the qualification exam; Prof. Camilla Karla B. Q. M. de Oliveira, Dr. Luana Wouk de Menezes and Dr. Maiara Bassi.

The referee panel for the PhD thesis is formed by a formidable group of researchers. I would like to thank Prof. Antonio Ferreira, Prof. Maria Luiza Rocco, Prof. Marcela Mohallem Oliveira, Prof. Marlus Koehler, Prof. Guinther Kellermann and Prof. Carolina de Matos Jauris for accepting to take part at the referee panel and for their comments to this work.

"For tomorrow may rain, so I'll follow the sun"

Lennon & McCartney

RESUMO

Dispositivos fotovoltaicos orgânicos (OPV) têm sido estudados por mais de 30 anos, mas só recentemente estão disponíveis comercialmente. Com a comercialização de módulos solares baseados em OPV surge a necessidade de avaliar seu desempenho em condições reais de uso. Nesta tese foi proposta a instalação de painéis OPV no topo de uma estação de ônibus tubular, que é um projeto urbano original da cidade de Curitiba. As estações de ônibus tubulares foram criadas na última década do século 20 e, na época, foram elogiadas por seu design inovador. Nos últimos anos as estações têm sido criticadas por falta de conforto térmico e excesso de consumo de energia. A instalação de módulos OPV torna as estações mais sustentáveis em termos energéticos, mantendo o seu design original, visto que os painéis solares são impressos em substrato flexível. A avaliação de desempenho dos módulos OPV disponíveis no mercado já foi realizada por outros grupos, mas não para o mobiliário urbano no sul do Brasil. Nesta tese, o desempenho e a resiliência dos painéis OPV foram avaliados por mais de um ano. Outro aspecto avaliado foi o acúmulo de sujeira nos módulos OPV e o efeito da sujeira no desempenho dos painéis. Há extensa literatura sobre o efeito da sujeira em módulos solares baseados em Si, mas nada em módulos OPV. À medida que a comercialização de painéis OPV aumenta, é importante entender como a sujeira afeta o desempenho dos painéis e encontrar maneiras de mitigar o problema. Com uma análise abrangente da eficiência e degradação dos módulos OPV em condições reais de uso, esta tese tem como objetivo preencher uma lacuna sobre o assunto e preparar o terreno para mais pesquisas na área.

Palavras-chave: OPV, mobiliário urbano, estação-tubo, sustentabilidade urbana

ABSTRACT

Organic photovoltaic (OPV) has been studied for more than 30 years but only recently it has been commercially available. With the commercialization of OPV based solar modules comes the need to evaluate their performance in real use conditions. In this thesis, I proposed the installation of OPV panels on the top of a tubelike bus station that is an original urban design of the city of Curitiba. The tubelike bus stations were created in the last decade of the 20th century and were praised for their innovative design. In the last few years, the stations have been criticized for lack of thermal comfort and excess energy consumption. The installation of OPV modules makes the stations more energy sustainable while keeping their original design as the panels are printed on a flexible substrate. Performance of commercially available OPV modules was done before by other groups but not for urban furniture in the south of Brazil. In this thesis, the performance and resilience of OPV panels were evaluated for over a year. Another aspect that was evaluated was soiling accumulation on the OPV modules and the effect of soiling on the performance of the panels. There is extensive literature on the effect of soiling on Si based solar modules but nothing on OPV modules. As the commercialization of OPV panels increases, it is important to understand how soiling affects the panels and to find ways to mitigate the problem. With a comprehensive analysis of the efficiency and degradation of OPV modules in real use conditions, this thesis aims to fill a gap on the subject and lay the ground for more research in the area.

Keywords: OPV, urban furniture, tubelike bus station, urban sustainability

List of Figures

List of Abbreviations

EDS	**E**nergy-**d**ispersive X-ray **s**pectroscopy
HOMO	**H**ighest **O**ccupied **M**olecular **O**rbital
ITO	**I**ndium **T**in **O**xide
LUMO	**L**owest **U**noccupied **M**olecular **O**rbital
OPV	**O**rgani **P**hoto**v**oltaics
OSC	**O**rganic **S**olar **C**ells
P3HT	**P**oly(3-hexylthiophene-2,5-diyl)
PCBM	**P**henyl-C61-butyric acid methyl ester
PEDOT	**P**oly(3,4-ethylenedioxythiophene)
PET	**P**olyethylene terephthalate
PSS	**P**olystyrene sulfonate
PV	**P**hoto**v**oltaic
SDG	**S**ustainable **D**evelopment **G**oals
SEM	**S**canning **E**lectron **M**icroscopy
UFPR	**U**niversidade **F**ederal do **P**araná
UN	**U**nited **N**ations
URBS	Urban planning administration
XPS	**X**-ray **P**hotoelectron **S**pectroscopy

Contents

Thesis outline

This thesis reports the efficiency and resilience of commercially available OPV modules installed over the stainless steel roof of a tubelike bus station in Curitiba. The bus station that was the object of study was donated to the university by the Curitiba's city hall and is located at the Centro Politécnico campus of UFPR. The work presented here report experiments done between 08/2018 and 11/2020.

Five chapters make up this work. The first chapter brings the motivation and a brief introduction to OPV. In the second chapter there is a literature revision on OSC and effect of soiling on PV modules.

The third chapter brings information on the installation of the OPV modules, the measurements done and also a discussion of the results. The chapter is divided in four sections that encompass all the techniques and protocols developed.

In the fourth chapter the main conclusions of the thesis are presented while in the fifth chapter ideas for future works are listed.

It is worth noticing that the bibliography of this thesis follows the model proposed by UFPR library. The references follow alphabetical order of the surname of the first authors.

Chapter 1

Introduction

1.1 Motivation

The 2030 agenda for sustainable development was adopted by all United Nations (UN) members in 2015. At the core of the agenda are the sustainable development goals (SDG) that call all countries for action to guarantee a prosper and peaceful future for all. The SDGs tackle the biggest challenges nations have to overcome to guarantee a better future for all. End of poverty, reduction of inequality, better health and better education are all listed as essential for sustainable economic growth [50]. The climate crisis and the preservation of forests and oceans are also issues addressed by the SDGs. Affordable and clean energy is SDG number 7, this goal has two targets; ensure universal access to affordable, modern and reliable energy by 2030 and increase substantially the share of renewable clean energy in the global energy mix [49].

The installed capacity of hydroelectric power in Brazil in 2019 was approximately 110 GW and represents around 70% of the total generation capacity of the country[44], [48]. Although hydroelectric power generates energy without carbon emission, the environmental cost of building dams is high. Another setback of hydroelectric power is the fact that the installed capacity reduces during dry seasons. The forecast for hydroelectric capacity is that the additions show be significantly lower than in previous years.

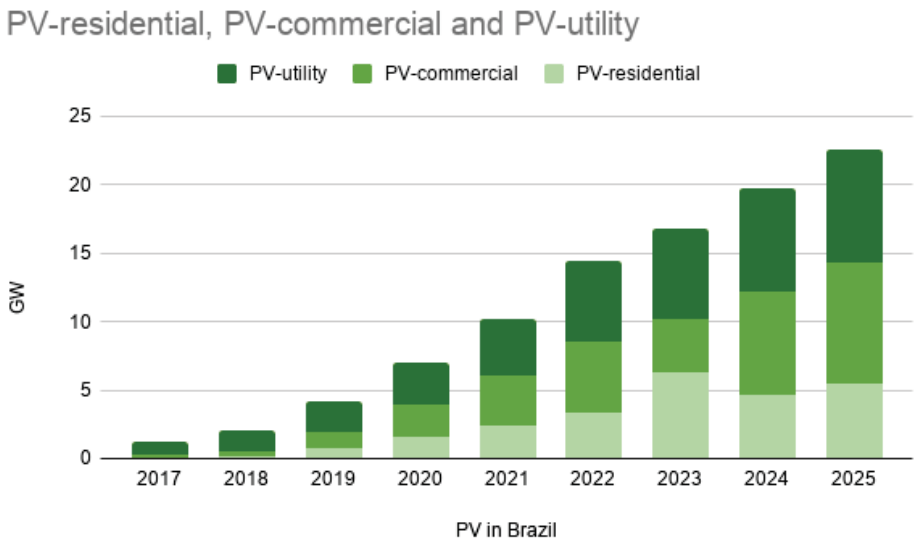

FIGURE 1.1: PV installed capacity in Brazil, font:IEA

The economic crisis plays a role in this scenario but also other energy sources are starting to get more attention from utility companies, commercial buildings and residences. Investment in photovoltaic (PV) energy generation is a promising way of improving the installed capacity in Brazil while keeping the energy matrix clean.

The market for PV energy in Brazil is still incipient but it should grow fast in the next few years, especially if the country manages to overcome the economic crisis that is taking a toll in most sectors of the Brazilian industry. IEA forecast for PV in Brazil says that the installed capacity in 2025 should be about 20 times the capacity the country had in 2017 [23]. In Figure (1.1) Minas Gerais, Rio Grande do Sul and Sao Paulo are the Brazilian states leading the initiatives on distributed PV energy in Brazil. Prices of utility-scale energy are regulated in Brazil by Câmara de Comercialização de Energia Elétrica (CCEE), in the last 3 years the government auctions price was lower than the unregulated market price for utility scale PV energy [13] [23]. This shows that the Brazilian market is demanding more PV energy.

With the increased interest in PV energy, the study of different solar technologies and their performances is necessary to better inform governments and general public about them. For more than 50 years solar technologies have been around. The last 30 years saw these technologies dramatically improve. With lower cost and higher efficiency, PV energy is attractive to residential and commercial consumers as well as to utility companies. In the United States in 2010 the cost of PV energy for residential consumers was 28¢, in 2017 the price dropped to 5¢for final consumers [4] .

The efficiency of solar cells improved for all solar technologies. Silicon (Si) based solar panels have been in the market for decades and are the most common solar technology. Consumers can find Si based solar panels with efficiencies around 20% (polycrystalline Si modules) and around 25% (monocrystalline Si modules), [15] .

Other Si based solar technology are the multijunction cells that have been around for more than 40 years and acchieve nowadays over 45% in efficiency. Multijunction solar cells are used mainly to power satellites and spacecraft because of their high cost [36].

Thin film based solar cells exist since the late 70's when their efficiency was less than 5%. Nowadays thin film cells with CGS and CdTe cells have efficiencies around 24% [36]. Organic photovoltaic (OPV) is a thin film technology that is based on organic composites to convert light into electric energy. In the past 30 years it went from solar cells with an efficiency lower than 1% in the end of the nineties to 18% in 2020, [36][22], see Figure 1.2.

Organic photovoltaic (OPV) is also a low cost technology and is easy for architectural integration as the modules are flexible and can be mounted on curved surfaces. OPV based panels can be printed on flexible substrates such as polyethylene terephthalate (PET) and can be produced using roll to roll

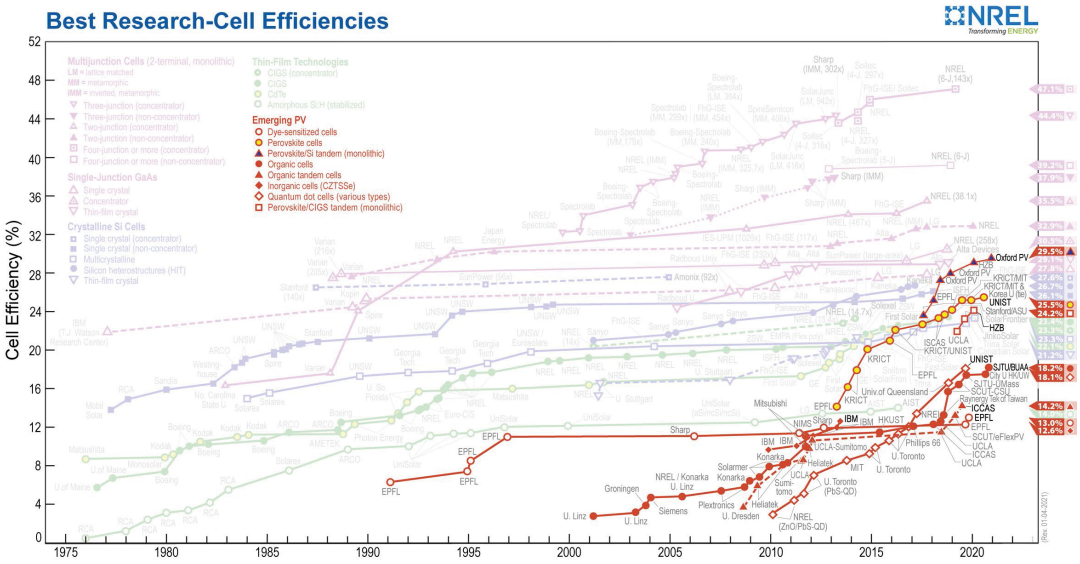

FIGURE 1.2: NREL chart highlighting emerging solar technologies. OPV efficiency increased rapidly from 2010. In 2020 an efficiency of 18.2% was reached in lab.

printing [45] - in a process that is similar to the way newspapers are printed. Because of the facility with which OPV panels can be integrated to urban furniture we chose these panels to install to install on a tubelike bus station (figure 1.4) that was designed 30 years ago for the city of Curitiba [38].

Integrate solar technologies is interesting not only because of the importance to put to test the said technology under real use conditions, but also for science dissemination. With around 800.000 people passing by the tubelike stations everyday, it is hard to think of a better platform to show society an emerging solar technology in use.

Before the Urban Planning Administration (URBS) decides to install OPV panels on tubelike stations that integrate the bus rapid transit (BRT) network in Curitiba, it is necessary to learn how the panels will work out of the lab environment, (figure 1.3). The main motivation for this thesis was to test OPV panels on a tubelike station that was donated by URBS. In October 2017 the station arrived at Centro Politécnico, UFPR campus where the Engineering and the Physical Sciences colleges are located (figure 1.4). The commercially

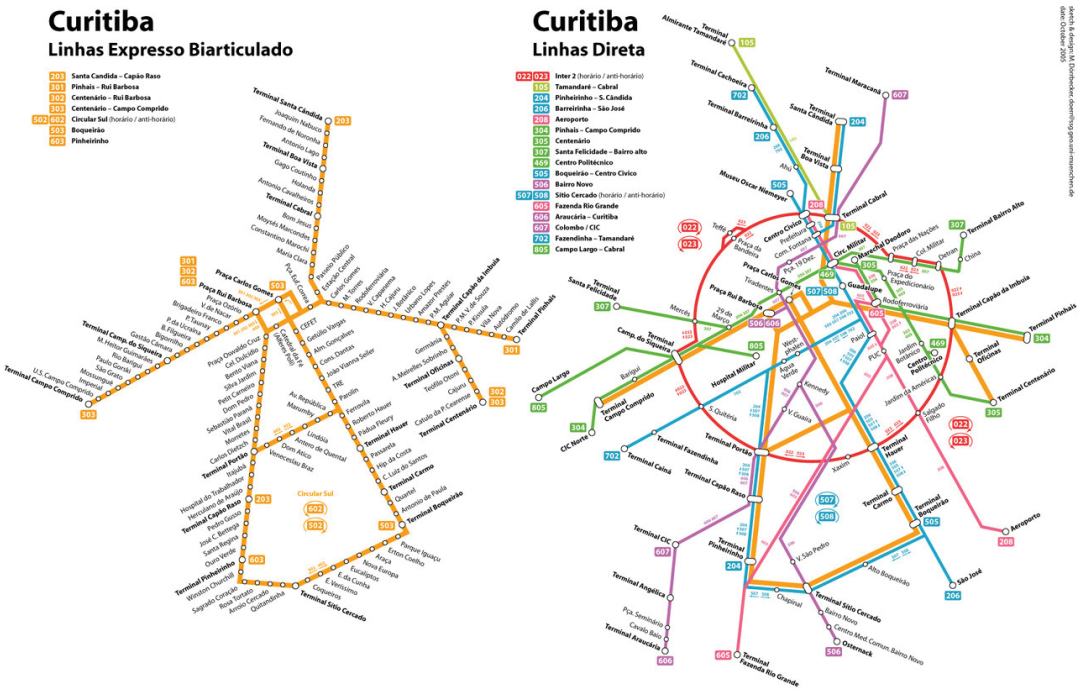

FIGURE 1.3: Map of the bus rapid transit network in Curitiba, dots indicate tubelike stations, font:URBS

available OPV panels were donated in June/2018 and then installed on the roof of the station. An electrical project was developed at low cost and the OPV modules started to operate.

The first measurements on the OPV panels started in August/2018 and continued for the next 2 and a half years. Those measurements told us about the efficiency and resilience of the OPV panels. In the next pages I report the measurements, materials and how OPV panels work.

1.2 Thesis Timeline

The purpose of this thesis is to showcase the use of OPV modules on urban furniture. Guided by the motivation to make solar technologies available to the wide public, the project to install OPV panels on a tubelike bus station was presented to the Engineering and Materials Science graduate program

FIGURE 1.4: Tubelike station donated by URBS at Centro Politécnico/UFPR. OPV panels installed on the roof of the station

(PIPE) . After the project was accepted in March/2017, the next step was to get a tubelike bus station.

Months of discussion with URBS to have all the legal and logistics aspects figured culminated with the tubelike station being delivered in October/2017. The station was installed on the same spot that a former station was, located at UFPR's Centro Politécnico campus. The previous station was an active one, used mainly by the UFPR community. Our tubelike station was donated to be a research unit, no buses stop by it, it is not an active bus station (figure 1.5).

A new challenge awaited after the station was in place. We needed commercially available OPV modules. In a dialogue with Sunew, the company that produces OPV panels in large scale in Brazil, we learned that there was a company, JSchebly, that would donate a few spare modules that they had bought from Sunew.

FIGURE 1.5: Tubelike station donated by URBS arriving at Centro Politécnico/UFPR.

It was then time to install the panels and design an electrical system to have the panels powering the station. The engineer of our research group developed a hybrid system that would power the station having the OPV modules as a source during the day and energy from the grid in the night time. The system also enabled temperature, light intensity and potential monitoring. A detailed description of the system is reported in [46].

With the bus station installed and the electric system working, measurements to evaluate the efficiency of the panels begun. In order to determine the efficiency of the OPV panels, several measurements to plot electric current versus potential (IxV) curves were done both in the dark and under sunlight. The measurements were done at different temperatures and different light conditions.

Apart from the IxV plots, an experiment to study soiling effect on OPV panels was developed. Microscopy and light transmittance measurements were done in samples under with varying times of exposition to soiling and different cleaning methods.

The measurements and experiments designed were done to help answer

the questions of how resilient and how efficient the OPV panels installed were. Only by answering those questions, it would be possible to develop a report to help URBS decide whether installing OPV panels on tubelike bus stations would be a good investment or not.

1.3 General Objective

- The purpose of this thesis is to showcase the use of OPV modules on urban furniture.
- Install OPV panels on a tubelike bus station.
- Answer the question of how resilient and how efficient the OPV panels commercially available are.
- Report the results to URBS.

1.4 Specific Objectives

In order to answer questions about the performance and resilience of OPV modules, there were few steps that had to be taken and protocols for the measurements also had to be developed. The work was divided in the following stages:

- Installation and connection of OPV modules
- Evaluation of the electric system
- Characterization of the OPV modules installed
- V_{OC} and I_{SC} measurements
- IxV measurements in the dark for all modules, to gather information on the degradation of the solar panels

- IxV measurements in the light for all modules, to gather information on the efficiency and other parameters of the solar panels
- Create and and execute a protocol to study how soiling affects on OPV modules
- Patent submission, utility model regarding the use of OPV modules on urban furniture, the case of the tubelike bus station
- Data analysis regarding IxV measurements
- Data analysis regarding transmittance and microscopy

Chapter 2

Literature Review

2.1 Operating principles of Organic Solar Cells

To generate power by the sunlight one should have a material that can absorb photons and induce charge separation. Then charge carries should make charge transport to the electrodes that will collect them, [20]. The absorption of the photon creates an excited state called exciton, this quasi particle diffuses within the material. When the exciton meets an internal electric field that causes the exciton, that is composed by an electron-hole pair, to separate. The opposite charges are then collected in the electrodes. This principle is similar to all PV cells, the photoactive materials used that are different for each type of solar cell. It is worth noticing that in Si based solar cells the excitonic effect is much larger than in OSC.

In organic solar cells, one can find in the active layer an electron acceptor material and an electron donor. The earlier OSC produced were based on a single component, later on bilayered and heterojunction OSC became more common. Fullerene based materials were the main acceptors used in OPV cells for a long time but recently nonfullerene materials have been successfully used in the active layer as electron acceptors, [32].

After incident light generates excitons (electron-hole pairs) at the electron donor material. The pairs are generated due to electron transitions from the π highest occupied molecular orbital (HOMO) to the $\pi*$ lowest unoccupied

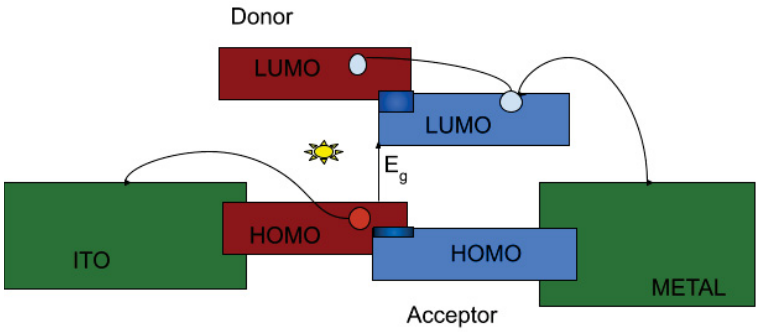

FIGURE 2.1: Drawing representing an OPV cell, sunlight is absorbed by a photon absorbant polymer. Electron donor layer in red and electron acceptor in blue.

molecular orbital (LUMO), as shown in (Figure 2.1). The absorption efficiency is linked to to the thickness of the donor material and to the optical absorption coefficient, [35].The binding energy of the exciton is less than the gap between the HOMO and LUMO bands ($\Delta G < E_{ex}$).

Inside the electron donor material the exciton diffuses until recombination of the exciton does not take place. Dexter electron transfer happens in short distances (0.2 to 3 nm) while Forster transfer happens in long distance (3 to 10 nm), [14]. Due to the thickness of the donor material layer, it is expected that part of the electron-hole pair recombine before the electrons are transferred to the acceptor material and the holes are collected by the ITO electrode.

2.1.1 Types of OPV cells

As previously mentioned, OPV cells can rely on a wide variety of materials for electron acceptor and electron donor layers. As the domain sizes of those layers are on the order of nanometers, excitons with short lifetimes are able

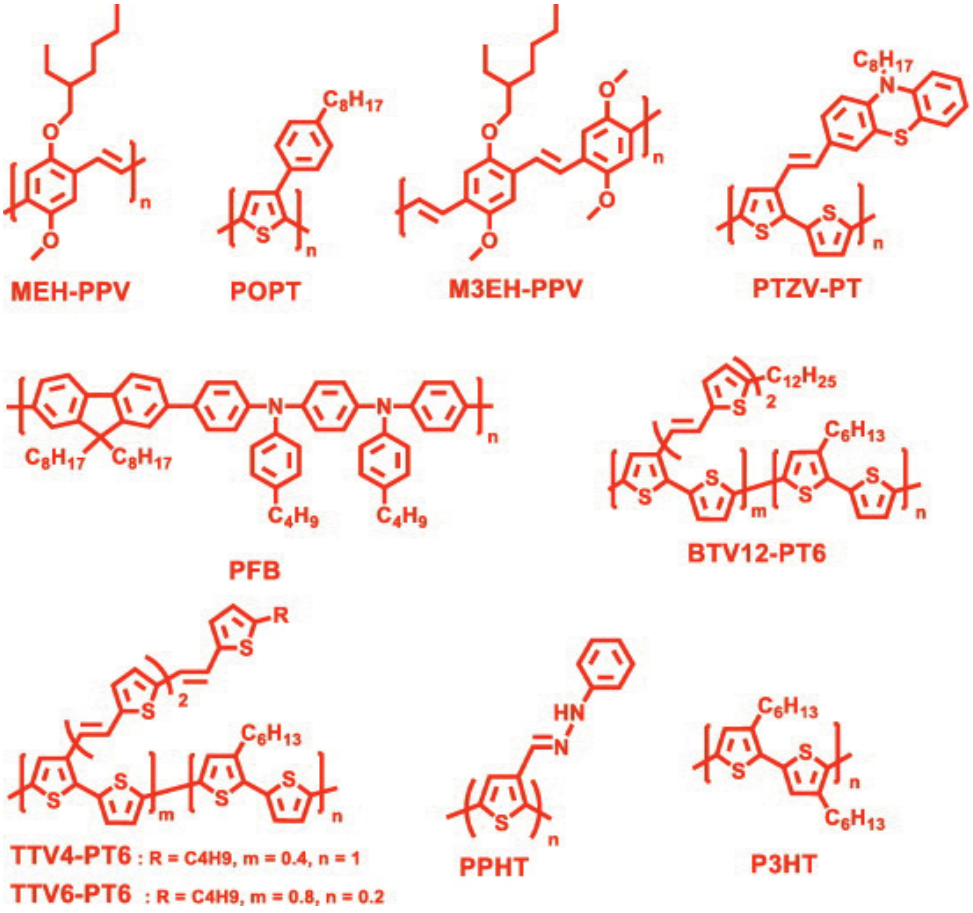

FIGURE 2.2: Donor materials used in OSC.©Antonio Facchetti

to reach an interface and dissociate because of the large donor-acceptor interfacial area. So, the cell itself does not need separated layers for donor and acceptor as it has in itself a number of electron acceptor and electron donor layers within it [42]. Heterojunction solar cells have been built for the past 30 years.

Through the years many different polymers were tested as electron donors in organic solar cells (OSC). Among the these polymers, those with thiophene group are commonly used, such as P3HT and those based on benzodithiophene terthiophene rhodanine (BTR), [17], [56], [6].

Fullerene based materials were used for many years as electron acceptors. Among fullerene based materials, PCBM - phenyl-C61-butyric acid

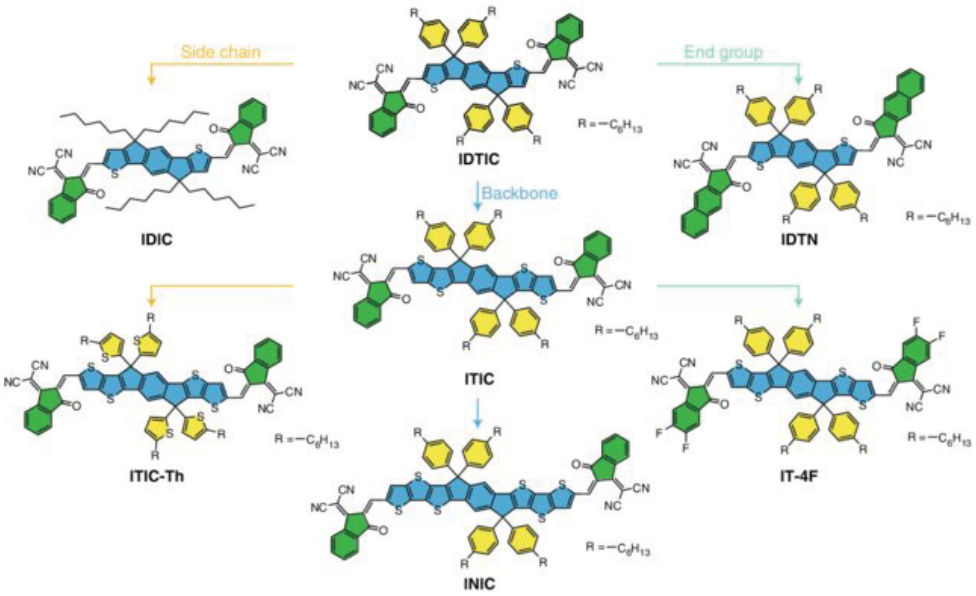

FIGURE 2.3: Some nonfullerene acceptor materials used in OSC.©Zhang et al./ Nature Energy, [57]

methyl ester ($C_72H_14O_2$)- has been widely used, [16]. Although the nonfullerene materials can result in highly efficient OPV devices, they present lower stability when compared to fullerene based cells as they start degradation process more rapidly, [10]. In Figure (2.2) the structure of a few donor materials, including P3HT, is shown while (Figure 2.3) shows the structure of some nonfullerene acceptors and Figure (2.4) shows the structure of a few commercially available fullerenes.

The active layer plays an important role in the OSC efficiency and stability, but there are other factors that affect the efficiency and resilience of an OSC. Both bulk heterojunction and bilayered devices present advantages and limitations. It is also possible to work with a blend of donor/acceptor plus a hole transport layer and an electron transport layer, [29], [53]. More recently

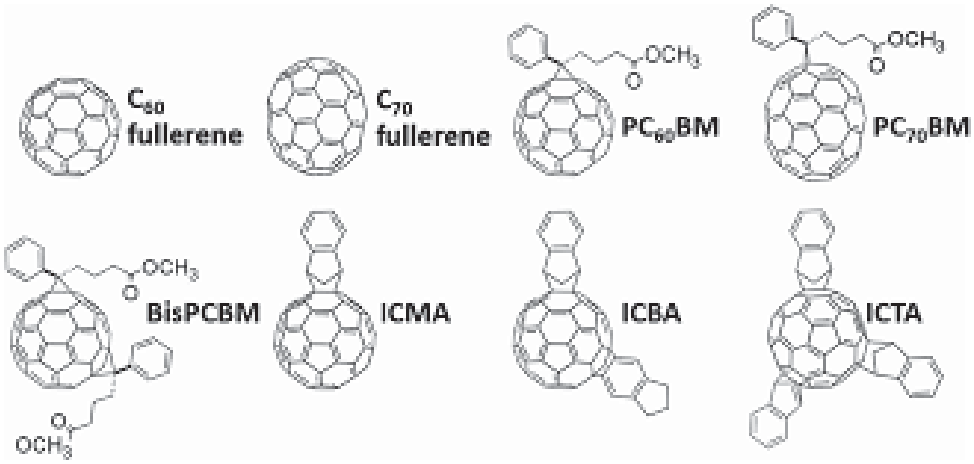

FIGURE 2.4: Fullerene acceptor materials used in OSC.©E.M. Speller/Materials Science and Technology

quaternary blends with donor-acceptor pairs mixed with donor and acceptor components were successfully used to build a device that achieved an efficiency of 18.03%, [55].

2.1.2 Optical and electrical losses in organic solar cells

In organic solar cells losses can occur in all steps of energy conversion. There are optical losses such as unabsorbed photons in the air-organic surface. At the nanostructural scale, excitation transfer might have losses if bimolecular recombination happens (reducing exciton diffusion yield) or at the interface - donor/acceptor interface or active layer/electrode interface. Electrical losses can happen in charge transport when electrons are trapped in defects in the active layer. These three types of losses affect the efficiency of OSC but there are ways to reduce them and optimize the cells, [33].

Appropriate thickness of the active layer helps to reduce optical losses. A layer with thickness around the diffusion length of the exciton allows higher diffusion efficiency, see Figure (2.5). The limitation that arises is that if the layers are too thin, the photovoltaic effect risks being reduced, [35]. The issue of too thin layers was solved with bulk heterojunction solar cells. In the case

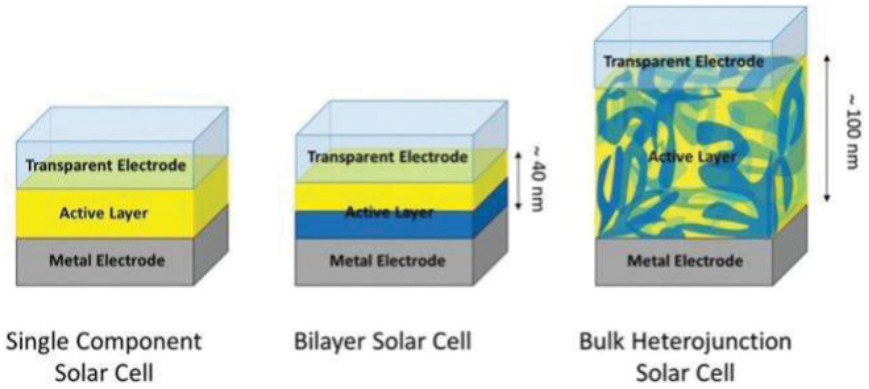

FIGURE 2.5: Design of OSC, while bilayer cells have a thickness of around 40 nm; bulk heterojunction cells are 100 nm thick.

of those, the main issue is charge carrier losses due to non geminate pair recombination [20], [51].

The transport of electron and holes through the material is made by charge carriers. Impurities inside the material and disorder within the material can trap the carriers as they react with these impurities, such as oxygen. The carriers can be trapped for a finite or infinite time. If carriers are trapped for a finite time, diffusion can still occur. When carriers are trapped for an infinite time then it compromises diffusion and the charge is not collected by the electrodes. A negligible defect density on the surface might be achieved with atomic layer deposition process. Then there will be a negligible number of available dangling bonds at the surface and impurities outside the material will not migrate to inside the cell or the electrodes, [2]. Trapping of charge carriers is one of the main causes of efficiency loss in PCBM based OSC, [5].

Mismatch between the HOMO-LUMO energy gap (E_g) and photon energy causes the excess energy to be dissipated as heat. On the other hand, if the energy of the incident photons is lower than E_g, the photon will not be absorbed. In Figure(2.6) the energy of the sun is plotted against the wavelength. In Figure (2.7) the photoresponse of an OSC with an active layer of

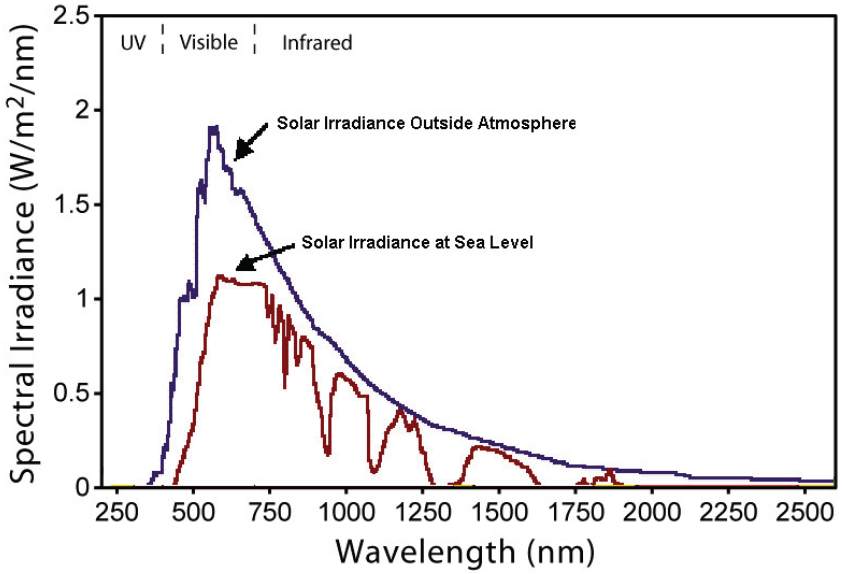

FIGURE 2.6: Solar spectrum, irradiance outside the atmosphere (in blue) and at sea level (in red), ©Luciano Mescia

P3HT:PCBM is compared to the solar spectrum, an abrupt decay in the photoresponse is observed at wavelengths higher than 650 nm, [27]. The area between the solar spectrum curve and the photoresponse of the P3HT:PCBM cell curve represents energy that will be dissipated as heat. In the area where the solar spectrum irradiance is below the photoresponse of the cell, the energy does not reach the HOMO-LUMO gap and the photons are not absorbed, and the photoresponse sharply decreases.

2.1.3 Parameters in organic solar cells

The power conversion efficiency (PCE) of a solar cell is determined by the open circuit voltage, V_{oc}; the short circuit current density, J_{sc}; and the maximum power, P_{max}. The open circuit voltage is the voltage developed when the two terminals of a cell are isolated. When the terminals are connected together the current drawn is the short circuit current, Isc. The ratio between

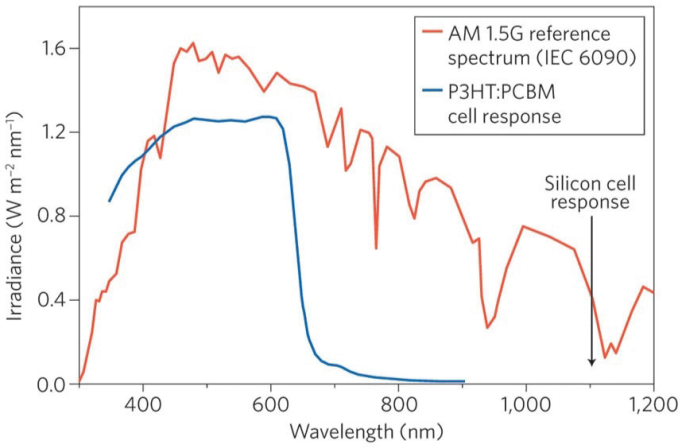

FIGURE 2.7: Comparison between solar spectrum and the photoresponse of a P3HT:PCBM solar cell. The P3HT:PCBM cell response drops at 650 nm while Si based cell response drops at 1100 nm. ©Nature Photon./Li et al.

the short circuit current and the area of the cell is Jsc. The maximum power of a characteristic curve corresponds to the point where the product of the voltage by the current reaches its maximum value, see Figure (2.9). From the definition of maximum power one can infer that the measurement and plot the current versus voltage is the characteristic way to extract P_{max} from the data. To calculate the efficiency, η, one should divide the maximum power by the power of the sun or the incident light (P_{in}), [37].

$$\eta = \frac{P_{max}}{P_{in}} \tag{2.1}$$

Another electric parameter in solar cells is the fill factor FF, that describes how square the JxV curve is. The value of the fill factor is associated to the facility or difficulty to extract carriers from the cell, by trapping and/or recombination and is given by 2.2.

$$FF = \frac{J_m V_m}{V_{oc} J_{sc}} \tag{2.2}$$

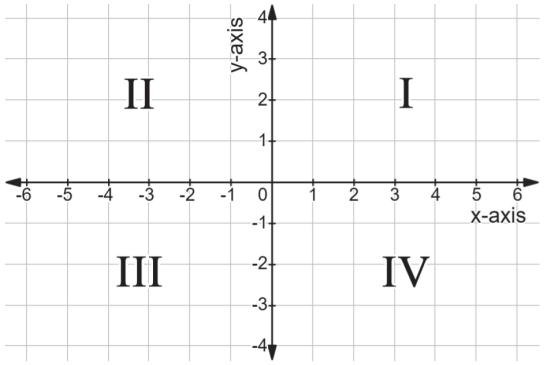

FIGURE 2.8: Quadrants of the coordinate system used in Figure 2.9 enumerated

The fill factor is related to the efficiency of a solar cell by substituting $P_{max} = J_m V_m$ for $J_m V_m = FF/[J_{sc} V_{oc}]$ in (2.2). The efficiency is then given by

$$\eta = \frac{J_{sc} V_{oc} FF}{P_{in}} \tag{2.3}$$

The graphic representation of the fill factor is the ratio between the areas of the rectangle given by $J_m V_m$ and the area of the rectangle given by $J_{sc} V_{oc}$, see (Figure 2.9). The upper limit of the P_{max} rectangle coincides with the JxV curve in the dark, while the values of J_m and V_m are given by the point where the JxV curve under illumination abruptly changes its angular coefficient, point where the first derivative is equal to zero.

The behaviour of the JxV curve in the dark changes depending on the intensity of the current. In a low current regimen, the current density varies as $J \propto \frac{V}{d}$, where d is the distance between the electrodes. This relation is due to the electrical properties of the electrode/organic interface, [35]. In a high current regimen the current density varies according to the Mott-Gurney law,

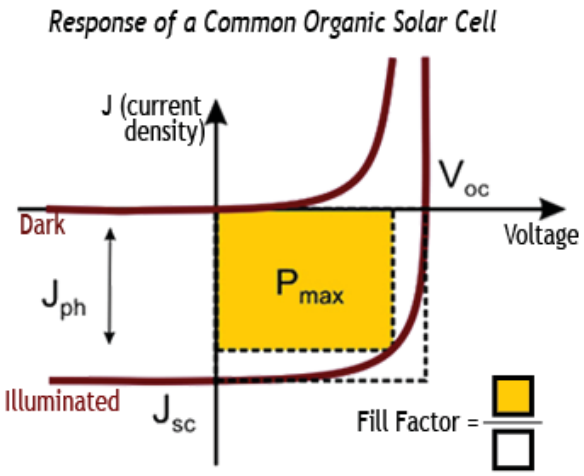

FIGURE 2.9: JxV characteristic curves of an ideal OSC in the dark and illuminated. Graphic representation of the fill factor(ratio between $P_{max}/(J_{SC}V_{OC})$),©MET/USC

as $J \propto \frac{V^2}{d^3}$. The behaviour of the diffusion current ($0 < J < 1.5$), is exponential, $(J \propto \exp \frac{qV}{kT})$. The different behaviours of the JxV curve in the dark are represented in (Figure 2.10).

The diffusion current in the IxV curve in the dark has exponential behaviour and can be fitted by the equation

$$I = I_0[\exp(\frac{qV}{kT}) - 1] \tag{2.4}$$

Under illumination a photocurrent (I_{ph}) appears and equation (2.4) becomes

$$I = I_0[\exp(\frac{qV}{kT}) - 1] - I_{ph} \tag{2.5}$$

A phenomenological explanation of the mobility of charge carriers of an OSC in the dark is explained in [26]. Degradation of OSC can also be observed looking at JxV curves in different dates. In Chapter 3 a degradation analysis using JxV curves in the dark is shown.

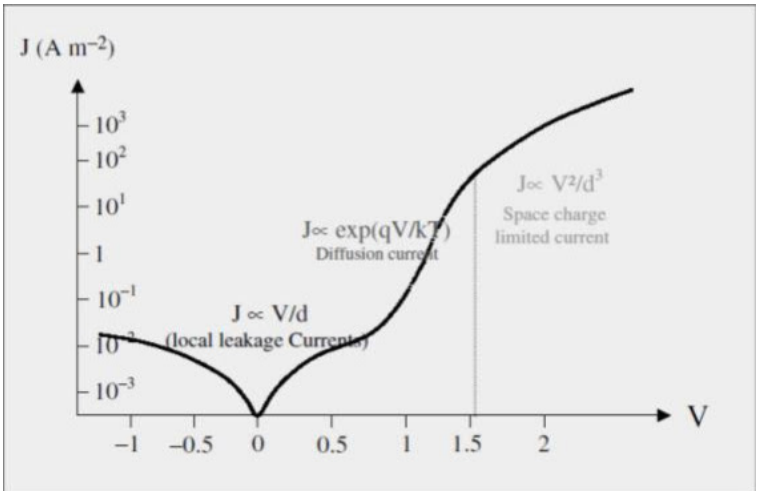

FIGURE 2.10: JxV curve in different behaviours. The V^2 dependance is reached only when the traps are shallow or there are no traps. ©Nunzi et al. [35]

Analysing the JxV curve under illumination, it is possible to see that the curve does not pass through the origin in the first quadrant, see Figure (2.9) and Figure (2.8), and $V > V_{oc}$. In the third quadrant the photocurrent approximates to the short circuit current ($J \rightarrow J_{sc}$), while $V \rightarrow 0$. In the fourth quadrant the the product of the current by the voltage is always negative meaning that energy is being produced by the OSC. The value of J gradually increases until it reaches J_m when it starts to rapidly increase, while V remains almost constant.

2.1.4 Equivalent circuit to a solar cell

The cell can be thought of as a current source where I_{ph} is a reverse current proportional to the incident light in parallel with a diode in the dark, see Figure 2.11. The voltage when the terminals are isolated - infinite load resistance - is V_{oc}. When the terminals are connected together the current is the short circuit current, I_{sc}. If the load resistance has a value between zero and infinite, $0 < V < V_{oc}$, and $V = R_L I$, where R_L is the load resistance, [35] [37]. The current delivered by the cell in the dark is that of a diode, given by equation 2.4. When the device is illuminated the current is then given by

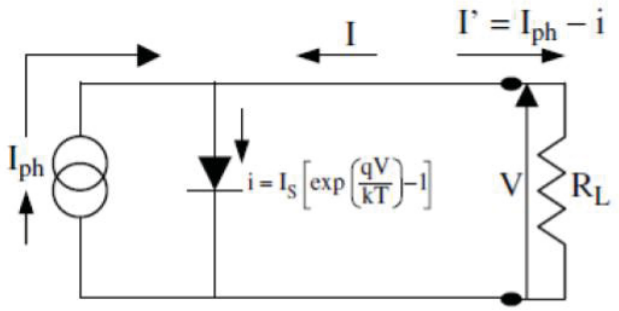

FIGURE 2.11: Equivalent circuit to an ideal solar cell. The two circles represent the cell that generates a current I_{ph} when illuminated. ©Nunzi et al. [35]

equation 2.5. The graphic representation of this circuit is shown in (Figure 2.11).

In a real OSC, the electrode/material interface gives rise to a resistance and one must also consider the metal resistivity in the electrode. Apart from those, there is also the resistivity in the bulk material, the more thick the active layer, more resistive it will be. When these resistances are not neglectable when compared to the load resistance, a series resistance (r_s) must be included in the equivalent circuit. The voltage in the presence of the series resistance is then

$$V = V_j - r_s I \tag{2.6}$$

Where V_j is the tension in the diode. Substituting V in equation 2.5,

$$\begin{aligned} I' &= I_{ph} - I_0[\exp\frac{qV_j}{kT} - 1] \\ &= I_{ph} - I_0[\exp(\frac{q[V + r_s I']}{kT}) - 1] \end{aligned} \tag{2.7}$$

where I' is the current in the diode.

When current leaks through the cell, around the edges of the device for example, a parallel or shunt resistance must be included in the equivalent circuit. The ideal situation happens when the series resistance is as small as

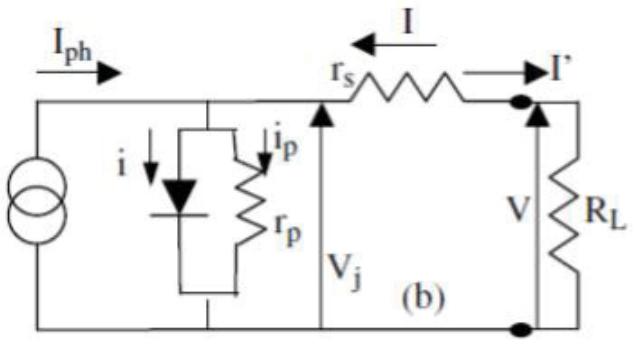

FIGURE 2.12: Equivalent circuit to a real solar cell. The two circles represent the cell that generates a current I_{ph} when illuminated. The load resistance is R_L, the shunt resistance is r_p and the series resistance is r_s. ©Nunzi et al. [35]

possible and the shunt resistance is as large as possible. The current in the presence of both resistances is given by

$$\begin{aligned} I' &= I_{ph} - i - i_p = I_{ph} - I_0[exp(\frac{qV_j}{kT}) - 1] - \frac{v_j}{r_{sh}} \\ I' &= I_{ph} - I_0[\exp(\frac{q[V + r_s I']}{kT}) - 1] - \frac{V + r_s I'}{r_{sh}} \end{aligned} \tag{2.8}$$

where $V_j = V + r_s I'$.

The equivalent circuit of a real OSC is represented in Figure (2.12). When the cell presents defects such as porosities on the surface that lead to a leak current across the whole cell, a second resistor should be added to the equivalent circuit. The effect of this second resistor (r_{p2}), is to cause a reduction on V_{oc} of a factor $\frac{r_{p2}}{r_{p2} r_s}$, [35]. In (Figure 2.13) the equivalent circuit with a second resistor in parallel is shown.

The code we work with at the lab to fit IxV curves tests a model with r_{sh} and r_p and another one with a second resistor in parallel. The model that gives the best fit to the data is the one used to calculate the parameters of the OSC.

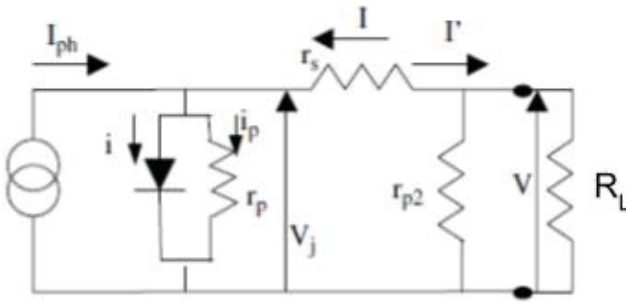

FIGURE 2.13: Equivalent circuit to a real solar cell with a second resistor in series. The two circles represent the cell that generates a current I_{ph} when illuminated. The load resistance is R_L, the shunt resistance is r_p and the series resistance are r_s and r_{s2}. ©Nunzi et al. [35]

2.2 Effect of soiling on solar modules

For more than 50 years it is known that soiling can affect the efficiency of solar modules. Soiling can reduce the efficiency of a module in more than 50% and it can also accelerate the degradation process of the cell. Although the literature on soiling effect on PV modules is extensive, little is published regarding how soiling affects organic PV modules and other thin film based solar technologies. In fact, no literature reference on soiling effect on OPV based modules was found. The protocols presented in this thesis were based on existing literature for *Si* based modules. In this section the literature on soiling effect on PV *Si* modules is revised.

The effect of soiling on a PV module is similar to the effect of a shadow. Different sizes of dust generate different kinds of shadow on PV modules. Air pollution generates a soft shadow while solid blocks of dust accumulated on a module generates a hard shadow that completely blocks the sunlight, [30].

The amount and type of dust in different regions of the globe varies a lot.

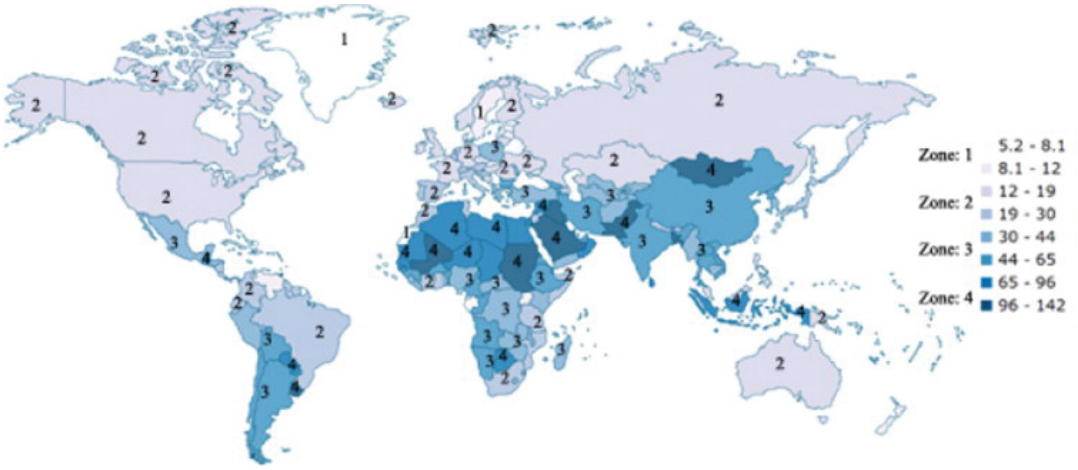

FIGURE 2.14: Dust intensity around the world. Places with higher amount of dust are darker than places presenting smaller amounts of dust, in $\mu g/m^3$, [18]

For this reason, it is important to know the local conditions in order to understand how a particular installation of PV modules will be affected by dust and how it is possible to mitigate such effects, [18]. In Figure (2.14) it is possible to observe the world map divided in 4 different degrees of dust intensity. The regions with higher amount of dust have up to 30 times more weight in dust per m^3 in the air than the regions with lower amounts of dust. Although Brazil has continental size, the whole country receives the same qualification regarding the amount of dust per cubic meter. Of course there are areas in Brazil that are more affected by dust than other areas, the scale presented in Figure (2.14) represents the average intensity of dust per country.

The composition of soiling and dust that accumulate on PV modules varies depending on the surrounding environment. In a big city, for instance, carbon based particulate material is common while close to plantations pollen particles abound. Characterization of soiling accumulated on solar modules has been the subject of many publications such as [7], [3] and [25]. One of the factors that characterization of soiling can help elucidate is the adhesion

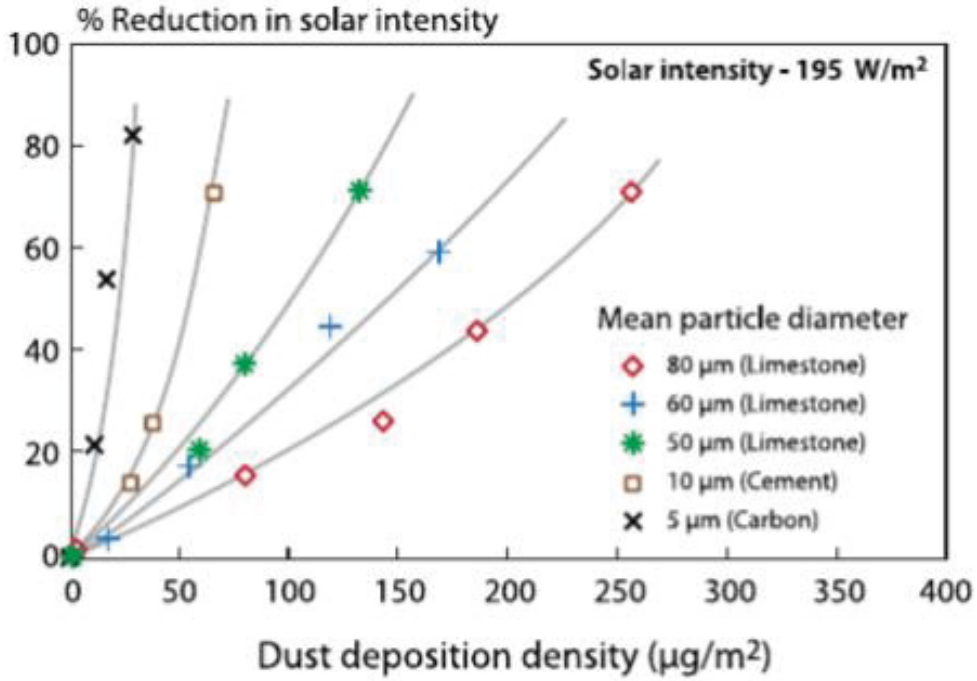

FIGURE 2.15: Reduction of solar intensity in presence of dust of different sizes [11]. Carbon smaller particles block sunlight more efficiently than limestone larger particles.

of different components to the module. Humidity is another factor that influences how strongly a component will bind to a surface, higher humidity means, in general, stronger adhesion, [30]. The size of the particles deposited on the surface also influences how strongly they will affect the performance of a PV module, [41] [11] [43].

The thickness of the dust layer accumulated on the surface of a PV panel also influences how the performance of such panel will be affected. The thicker the dust layer less sunlight hits the surface of the module and less energy is converted into electricity, [40]. When it comes to the size of the particles of the same composition, thinner particles block sunlight more effectively than coarser ones; causing a greater difference in the performance of PV modules affected by a thin particle layer. This happens because smaller

particles get closer together leaving less space in the interface between particles for the light to pass through.

Summarizing the main factors related to soiling that affect the performance of solar panels, we have

- Chemical composition of the dust accumulated,
- Size distribution of the particles in the dust,
- Density of the dust layer deposited on the surface.

To study the effect of these main factors on the performance of PV modules, it is necessary to combine different techniques. For instance, measuring light transmittance through the material that encapsulates the module; scanning electron microscope (SEM) to determine topography and composition of dust particles; IxV measurements to check differences in performance of a module with different amounts of soiling accumulated on it, [8] [25] [41].

Although there is extensive literature on how soiling affects the performance of Si based PV modules, little is know about soiling effect on OPV based modules. As this work accessed commercially available OPV modules, we understood that the work wouldn't be complete without accessing the effect of soiling. Because this thesis will be the basis for a white paper where the installation, performance and reliability of OPV modules will be described for Curitiba's city hall; it was necessary to develop a protocol for mitigation of soiling on OPV panels. The protocols developed and the techniques used to evaluate soiling effect on organic solar panels are described in Chapter 3.

Chapter 3

Materials, Methods & Results

3.1 Installation

In july 2018 the OPV modules were installed on the roof of the tubelike bus station. The application of the OPVs was made on a metallic surface (the roof is made of stainless steel) and was done according to the presented design. The OPV modules were ready for installation as they came with an adhesive coating. Each module has 32 OSC that are connected in series. After the solar modules were installed, the electrical connections had to be made. The modules were connected two by two in a common conductor, through MC4 connectors, according to the proposed design, forming 14 sets as shown in Figure (3.1). Each of the module sets ended up with 64 OSC connected in series (32 OSC in per module). In these sets, the negative terminal of the panel was connected in series, while the positive terminal, differing slightly from the project, was connected in parallel through a positive bus bar inside the distribution board, in order to allow the research and individual evaluation of each of the 14 panel sets. Since the sets are composed of only two panels in series and are connected in parallel, there was no need to install bypass diodes [37]. A picture of the roof with the modules installed can be seen in Figure (3.2) while the connections can be seen in Figure (3.3).

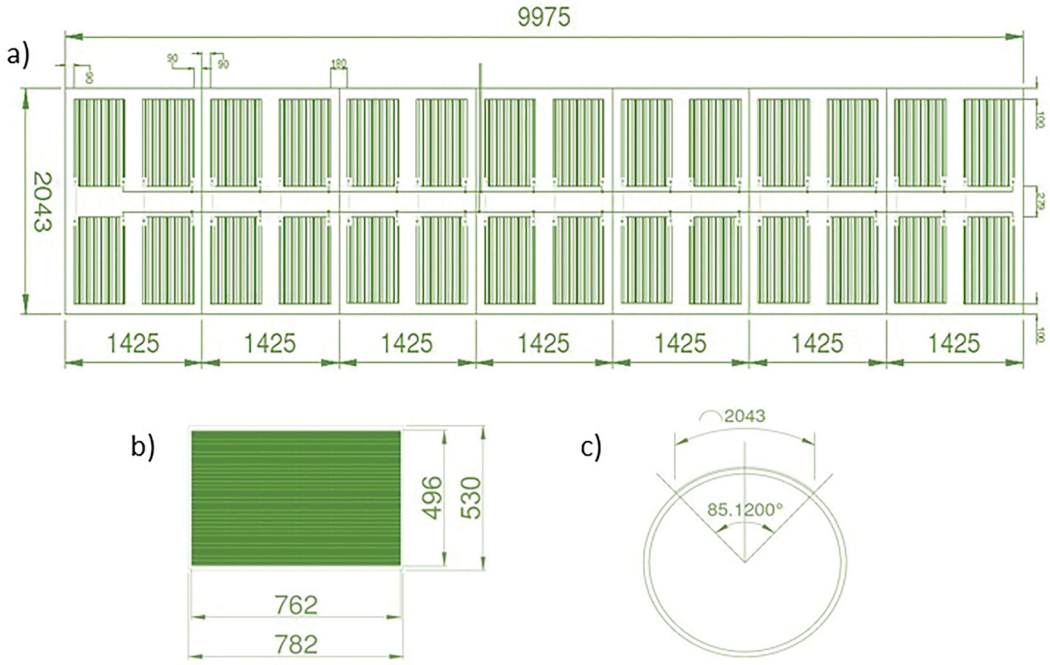

FIGURE 3.1: Design for installation of the solar modules made by ©Sunew. a) Installation design for 14 sets of modules with a spacing of 90 mm between them and a central conductor with 273 mm width. b) View of a single module that has 32 OSC connected in series. c) Frontal view of the tubelike station with a section of 2043 mm where the metal roof is placed.

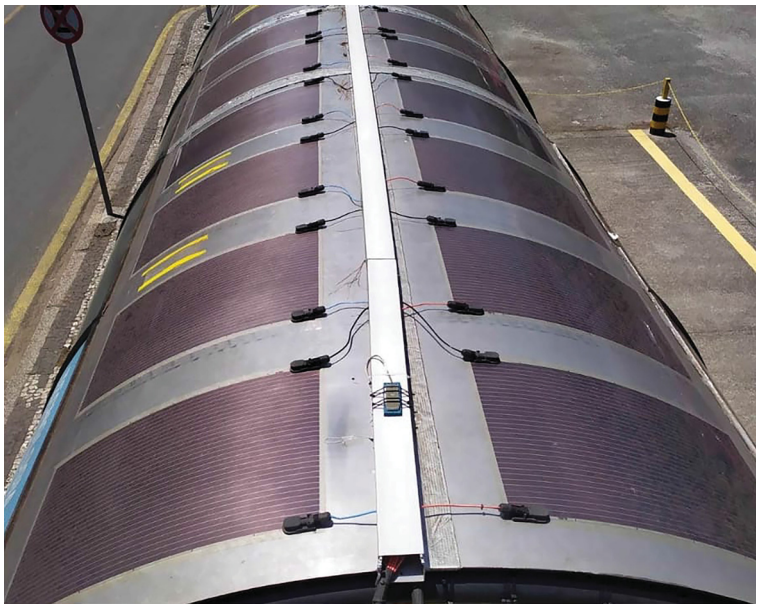

FIGURE 3.2: OPV modules installed on the roof of the tubelike bus station.

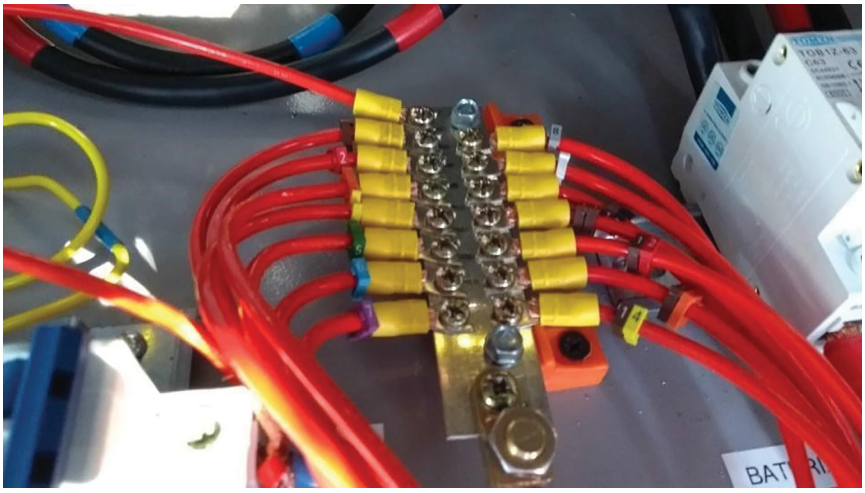

FIGURE 3.3: Connections for the 14 sets of solar modules

A distribution board was developed to control the energy generated by the OPV, store it in batteries, convert it back to AC, and protect and control the power supply between OPV/grid. Preferably, OPV modules will keep the tubelike bus station powered, if the OPV modules generate enough energy they will be the only energy source. The load can be transferred from the OPV modules to the grid during tests, research, or battery discharge. OPV and grid supplies enter through this board. In a common situation, the OPV will be supplying the charge controller during the day, with the voltage depending on the lighting level of the panels, which, in this case, can reach up to 54 VCC. The charge controller regulates this input voltage to an output voltage between 21 VCC, minimum discharge voltage for lead-acid batteries, and 29.4 VCC, maximum charge voltage for lead-acid batteries, charging the 24 VCC batteries [47]. In addition, the OPV modules also powers the voltage inverter, in parallel to the battery, which converts the 24 VCC input voltage to a 120 VAC output, supplying the loads of the tubelike bus station. A programmable timer that controls the automatic lighting of the tube station was also installed. Lighting of the station does not depend on which power

FIGURE 3.4: Front door of the distribution board. Green light on meaning the bus station is being powered by the OPV modules.

source (OPV or grid) is powering the load, its power supply and activation come from the power output to the load. The front panel of the distribution board, with the integrated electrical meters for voltage (V), current (A), power (W), and energy (Wh) measuring the OPV input and the inverter output can be seen in Figure (3.4). The green light "on" indicates that the OPV panels are supplying the system. Apart from lighting, 2 chargers were installed inside the bus station to charge cell phones via USB. Each charger can supply energy to up to eight mobile phones, see Figure (3.5). The main equipment that needs energy supply are the automatic doors, in the case of the tubelike bus station tested, the doors were open and closed just to test the system. The energy consumption for an $11m$ long tubelike bus station is, in average, $180kWh$ per month. The OPV modules installed were able to provide for 80% of that amount while their efficiency was around 1.5%.

The installation of the OPV panels on the roof of the tubelike bus station is explained on article [46]. The article is also available in annex 2. The utilization

FIGURE 3.5: Charger for mobile phones with 8 USB ports.

model of OPV panels for the tubelike station was deposited on June/2020 at the Brazilian National Intitute for Patents (INPI), see annex 1.

3.2 Characterization of OPV films

The physico-chemical characterization of OPV films gives information about the quality of the active layer film of the device. In this context, the analysis of the morphology, chemical composition and degradation of the films is important to evaluate the quality of the fabrication process. A collaboration with the research group led by Prof. Maria Luiza Rocco from UFRJ, allowed the samples to be analyzed by X-Ray Photoelectron Spectroscopy (XPS). The samples analysed were prepared by the same company that commercializes the OPV modules studied in this thesis and were taken out of the fabrication process just before the second electrode deposition would be done, see Figure (3.6). Although the supplier test the quality of the panels produced, their analysis is not published. As it is important to learn about the quality, characteristics and performance of the OPV modules installed on the tubelike bus station, XPS is a powerful tool for surface analysis, elemental composition and chemical states of the elements present in a sample.

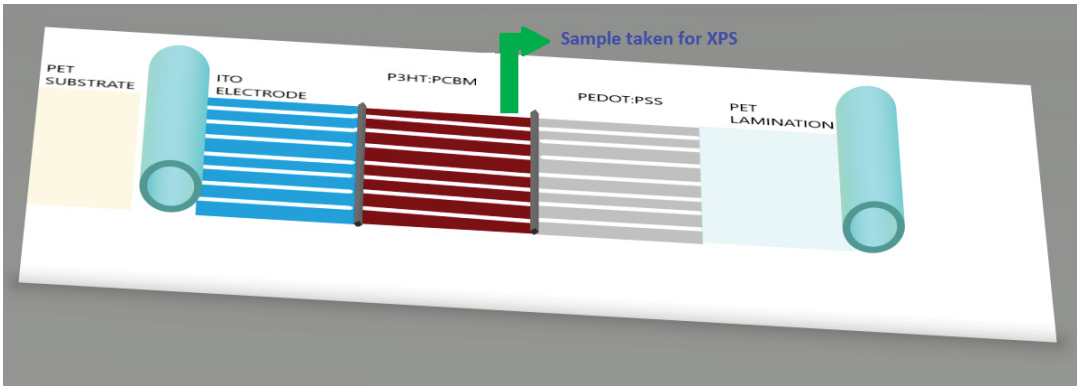

FIGURE 3.6: Illustration of the fabrication process of the OPV modules at Sunew. Each module has 32 cells connected in series. The sample for XPS was taken just after the active layer was deposited.

In the XPS analysis, information on chemical states and their concentration within the samples could be gathered. The equipment used to analyze the spectrum was a Thermo Escalab 250Xi spectrometer equipped with an $AlK\alpha$ X-ray monochromatic radiation ($h\nu = 1486.6$ eV) and a hemispherical electron energy analyser, see Figure (3.7). The pressure inside the vacuum chamber was maintained below $5x10^{-9}$ mbar.

The pass energy of the spectrometer was 100 eV and 25 eV for XPS survey and core level spectra, respectively. The XPS results were fitted by Gaussian and Lorentzian functions using the Avantage v.5.982 program and the binding energy scale was calibrated using $Au4f_{7/2}$ line at 84.0 eV.

In the case of the OPV modules installed on the tubelike bus station, the active layer film was based on P3HT:PCBM. The XPS survey spectrum of the film, the active layer was deposited over a flexible substrate. The spectrum displayed only peaks related to the expected elements (C, S, and O). As no impurities was found, it is safe to say that the quality of the deposited film was good and was free of contamination and impurities. The core level signals (C1s, O1s, S2s, S2p) are clearly visible, which are related to the thiophene units and the fullerene derivative. See Table 3.1 for information on the surface composition of all elements and their atomic percentage.

FIGURE 3.7: Thermo Escalab 250Xi spectrometer equipped with an AlKa X-ray monochromatic radiation ($h\nu$ = 1486.6 eV).©Thermo Scientific - Scientific Instruments and Aut

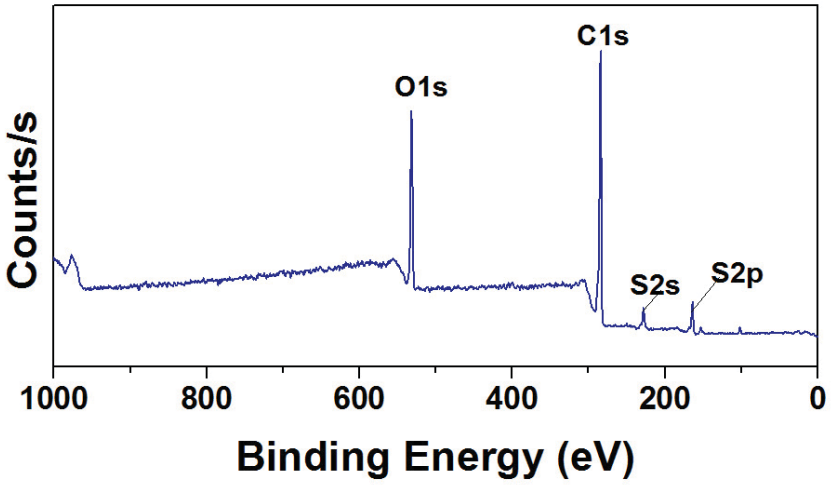

FIGURE 3.8: XPS survey spectrum of printed P3HT:PCBM film, done with Thermo Escalab 250Xi spectrometer equipped with an AlKa X-ray monochromatic radiation ($h\nu$ = 1486.6 eV).

TABLE 3.1: Surface composition of the P3HT:PCBM film in atomic percentage, done with Thermo Escalab 250Xi spectrometer equipped with an AlKa X-ray monochromatic radiation ($h\nu$ = 1486.6 eV).

Peak Assignment	Peak BE (eV)	Atomic (%)
C1S	284.5	75.4
O1S	532.0	19.2
S2P	164.1	5.4

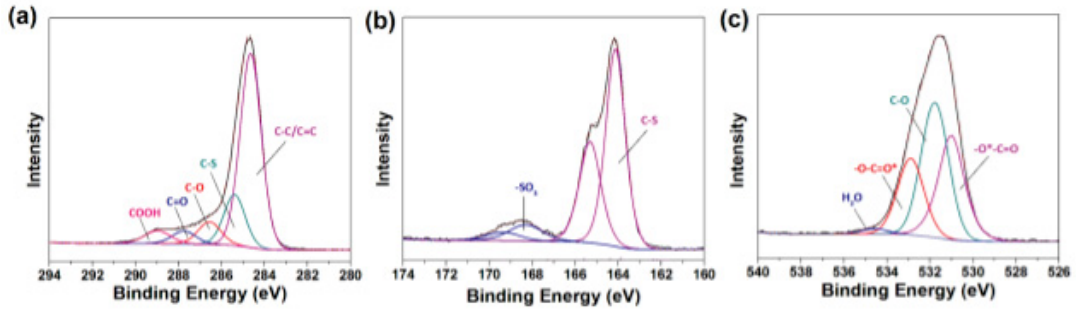

FIGURE 3.9: High resolution XPS survey spectrum of printed P3HT:PCBM film, done with Thermo Escalab 250Xi spectrometer equipped with an AlKa X-ray monochromatic radiation ($h\nu$ = 1486.6 eV)

High-resolution core-level spectra were obtained to further confirm the integrity of the film by analyzing the chemical environment of each element probed in the survey spectrum.The C1s core-level spectrum, which presents peaks related to the C-C/C=C bonds of thiophene and fullerene, peaks associated with carbon bonded to oxygen atoms due to the methyl esther group of the fullerene derivative (PCBM) and also the C-S bond, as expected by the presence of thiophene, see Figure 3.9. From the analysis of the S2p high resolution spectrum, it is possible to observe the main contribution of the C-S bond from the thiophene ring; a less intense feature at higher binding energy is also measured (secondary peak), most probably due to surface oxidation, which is common in organic materials. O1s high resolution XPS spectrum shows three major contributions, due to the fullerene derivative. The presence of a very low intensity feature at higher binding energy was associated with water. Peak assignments and atomic percentages of these core levels can be seen in Table (3.10).

Core Level	Peak Assigment	Peak BE (eV)	Atomic (%)
C1s	C-C/C=C	284.7	64.2
	C-S	285.4	17.1
	C-O	286.6	8.3
	C=O	287.8	5.0
	COOH	289.0	5.4
$S2p_{3/2,1/2}$	C-S	164.1	87.3
		165.3	0.00
	$-SO_x$	168.3	12.7
		169.3	0.00
O1s	-O*-C=O	531.0	32.6
	C-O	531.8	42.6
	-O-C=O*	532.9	23.2
	H_2O	534.6	1.6

FIGURE 3.10: C1s, S2p, and O1s peak assignment and atomic percentage for the P3HT:PCBM film, done with Thermo Escalab 250Xi spectrometer equipped with an AlKa X-ray monochromatic radiation ($h\nu$ = 1486.6 eV)

3.3 Current versus voltage measurements

As explained in Chapter 2, IxV measurements can give information on performance, parameters and degradation process of OPV modules. In this thesis, IxV measurements were done for 2 and a half years on the OPV modules installed on the tubelike bus station. This long term analysis gave information on the degradation process of commercial OPV modules under real use conditions. The usual way to present IxV data is to plot JxV curves, where J is the current density given by

$$J = \frac{I}{device\ cross\ section\ area} \tag{3.1}$$

The first set of measurements was done to compare the response of all 14 OPV modules. It was important to check the response for the case of defective modules or installation problems. All modules had similar response as can be seen in Figure 3.11.

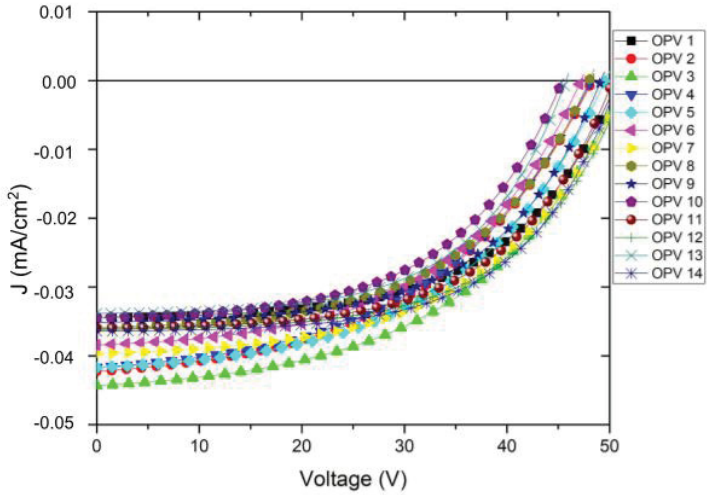

(A) JxV curves under sunlight, where J is the current density

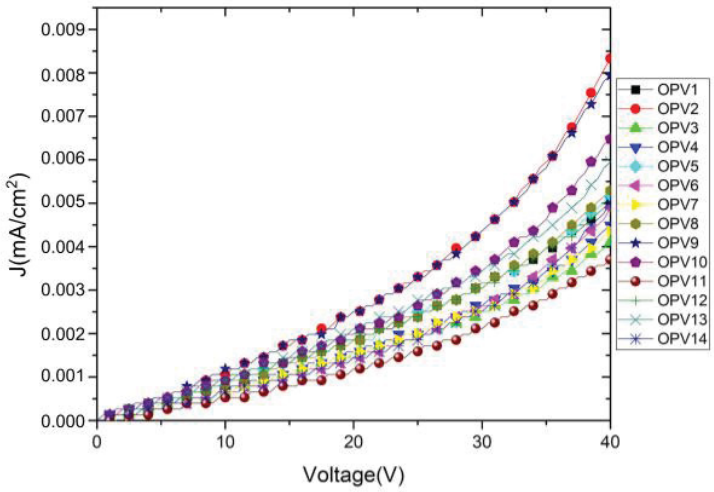

(B) JxV curves in the dark

FIGURE 3.11: JxV curves. Measurements done when the modules were installed, 3.11a under sunlight and 3.11b in the dark. The dispersion observed in the curves was expected due to several factors such as manipulation, amount of sunlight and installation

TABLE 3.2: Parameters of the OPV module, *after cleaning

Date	V_{oc} (V)	J_{sc} (mA/cm^2)	$R_{sh}M\Omega$	$R_sM\Omega$	$FF(\%)$	η (%)
08/31/2018	32.39	$1.66.10^{-2}$	3.91	1.1	33.81	1.54
11/30/2018	50.58	$3.42.10^{-2}$	524	0.186	64.72	1.51
12/05/2018	48.73	$3.43.10^{-2}$	64.4	0.217	58.32	1.38
04/12/2019	41.66	$2.56.10^{-2}$	16.6	0.415	48.98	1.07
09/12/2019	43.31	$3.09.10^{-2}$	4.64	0.826	34.27	0.74
10/10/2019	40.68	$3.88.10^{-2}$	2.55	2.39	32.10	0.72
10/25/2019	40.40	$4.73.10^{-2}$	1.27	3.90	28.26	0.8
12/11/2019	36.75	$4.36.10^{-2}$	1.06	1.06	22.56	0.51
11/20/2020	25.29	$2.48.10^{-2}$	1.77	1.77	20.04	0.18
11/20/2020*	26.37	$2.68.10^{-2}$	0.676	1.81	19.7	0.2

TABLE 3.3: Maximum power, illuminance (Il), and irradiation (Il x 0.0079), *after cleaning

Date	P_{max} (mW/cm^2)	Irradiance (mW/cm^2)	Illuminance (klx)
08/31/2018	0.2	13.05	16.5
11/30/2018	1.42	94	74.3
12/05/2018	1.24	90.2	71.26
04/12/2019	0.84	78.7	62.17
09/12/2019	0.58	78.1	61.7
10/10/2019	0.59	82.5	65.18
10/25/2019	0.68	85.3	67.39
12/11/2019	0.46	91	71.89
11/20/2020	0.16	88	69.52
11/20/2020*	0.18	90	71.1

After this first evaluation, a series of measurements was done under sunlight and in the dark for the next 2 and a half years. Parameters were calculated with a model that tested if it was necessary or not to add a second resistance, the model used for all calculations is the one presented at [35] and the equivalent circuits are shown in Figures (2.12) and (2.13). In Table (3.2) the parameters calculated for all dates for module 7 are listed, this module is located in a central position and is not shaded throughout the day by the building or the trees that are close to the tubelike bus station.

The degradation process can be observed in the JxV curves as the curves

go over time from an exponential to an "s" form and then to a straight line, see Figure 3.12.

JxV measurements were also done in the dark as these curves can elucidate if a degradation process is underway or if the curves under sunlight showed degradation features due to factors such as accumulated soiling on the modules, [26][25]. If there is a degradation of the active layer, it is expected that the angular coefficient of the curve diminishes as the degradation process happens. In the case of the OPV modules installed on the tubelike bus station, although some difference was notice in the linear plot see Figure 3.13; no visible difference was noticed in the loglog plot, see Figure(3.14). It is expected that the curves in the dark for a single cell are exponential. The measurements for the modules (comprising 64 cells each) are not the same, the plot is linear. As the color of all modules did not change over time, it is likely that the active layer did not degrade significantly over time.

Analysing the measurements done under sunlight and in the dark, it is clear that a degradation process started 8 months after the modules were installed. It is likely that the degradation was accelerated by the high temperatures that are reached at the stainless steel roof of the tubelike bus station. In a day with a maximum temperature of 30^{o}C, the roof can reach a temperature of 65^{o}C. In Figure (3.15) it is possible to see how the average temperatures varied from the date when the modules were installed until the last measurements were done 27 months after. Figure (3.16) shows the variation in humidity through the 27 months. It is known that high humidity, high light irradiation and high temperatures induce degradation is OSC, [21], [34]. As the average humidity in Curitiba is around 80 % per month, it contributed for the degradation of the modules. Another factor to be considered is the amount of UV light as PCBM tends to degrade faster in its presence.

In order to have a clearer comparison of the JxV curves measured under sunlight, plots of 3 measurements were taken from dates that were 12 months

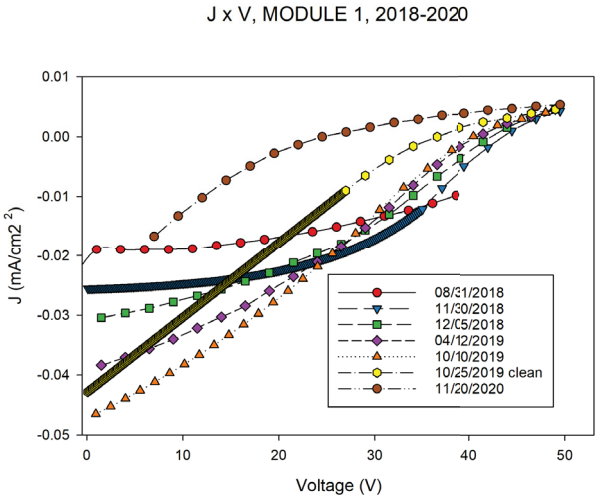

(A) Module 1 (closer to the distribution board), time series, JxV curves under sunlight

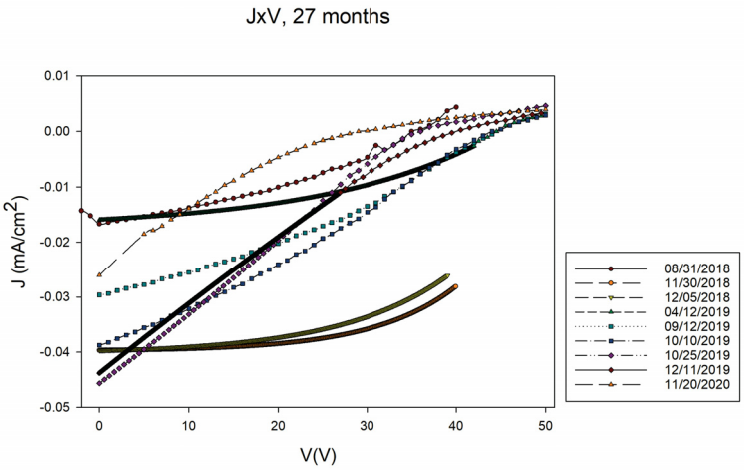

(B) Module 7(middle of the tubelike station), time series, JxV curves under sunlight

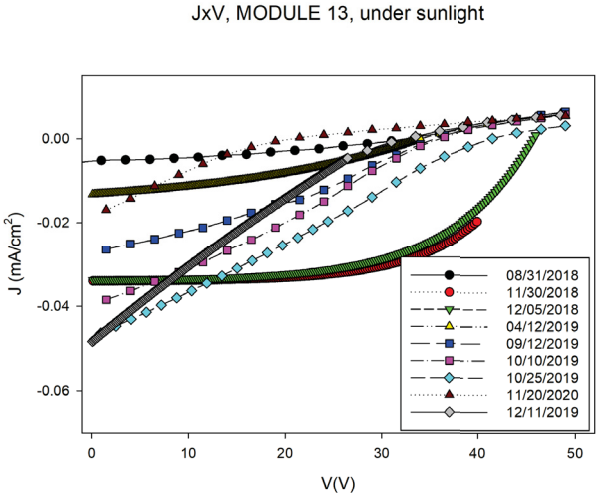

(C) Module 13 (end of the tubelike station), time series, JxV curves under sunlight

FIGURE 3.12: JxV curves under sunlight measured over 2.5 years. 3.12amore distant to the distribution, sunlight all day. 3.12b middle of the tubelike bus station, sunlight all day. 3.12c closer to the distribution, partially shadowed by trees

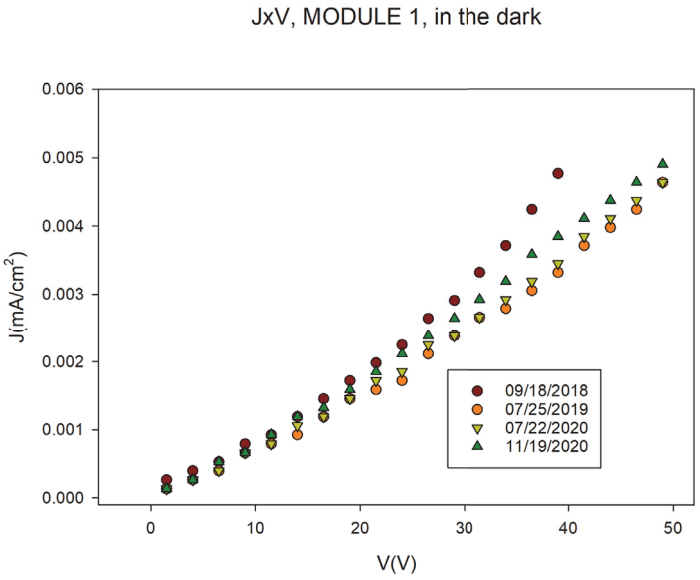

(A) Module 1, time series, JxV curves in the dark

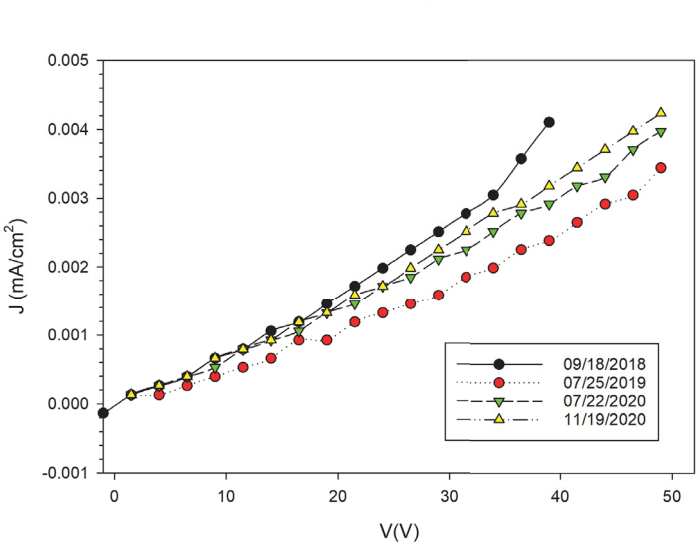

(B) Module 7, time series, JxV curves in the dark

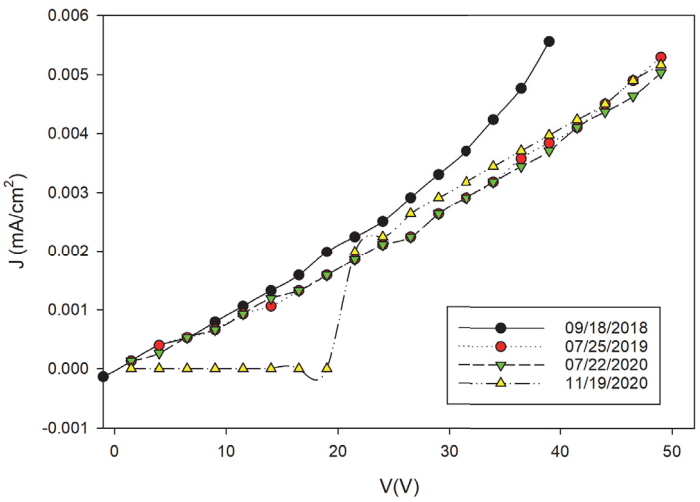

(C) Module 13, time series, JxV curves in the dark

FIGURE 3.13: JxV curves in the dark measured over 2.5 years.

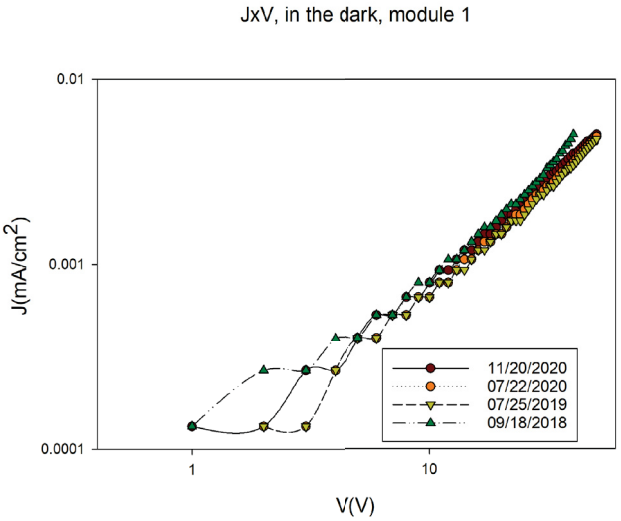

(A) Module 1, time series, JxV loglog curves in the dark

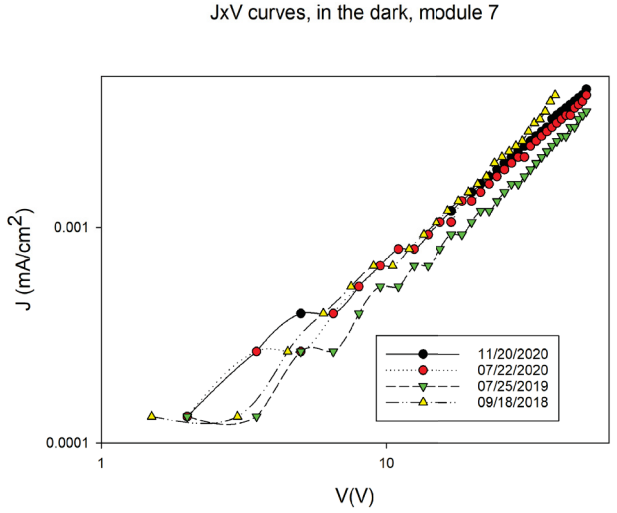

(B) Module 7, time series, JxV loglog curves in the dark

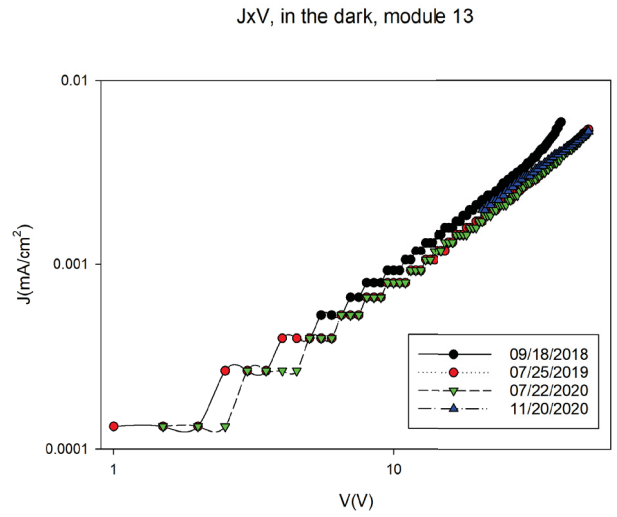

(C) Module 13, time series, JxV loglog curves in the dark

FIGURE 3.14: JxV loglog curves in the dark measured over 2.5 years.

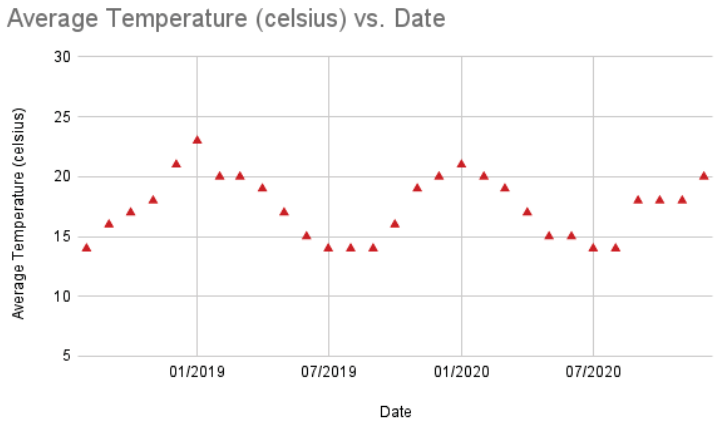

FIGURE 3.15: Average temperature - timeline in the 27 months window when the JxV measurements took place, data by INMET (https://portal.inmet.gov.br/).

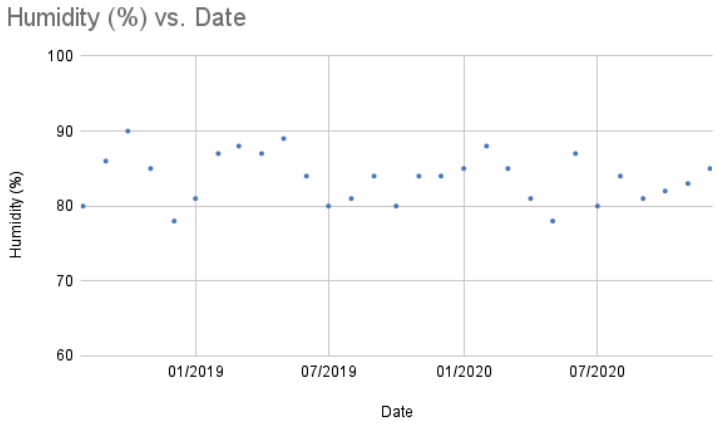

FIGURE 3.16: Average humidity - timeline in the 27 months window when the JxV measurements took place, data by INMET (https://portal.inmet.gov.br/).

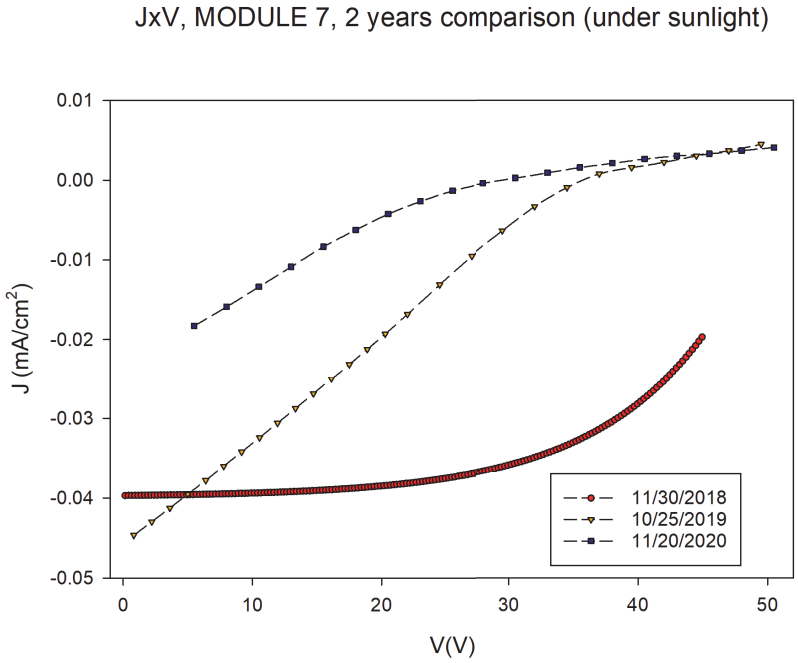

FIGURE 3.17: JxV curves under sunlight 3 months, 15 months and 27 months after the modules were installed.

apart from each other. Those plots show how the shape of the curves differ, see Figure 3.17. After one year the measurement shows clearly that a degradation process is underway, after 2 years the slope of the curve decreased showing that the degradation continued.

The analysis of the PV parameters calculated from the JxV curves, shown in Table 3.2, helps to understand how is the performance of the OPV modules and the degradation process they went through. The fitting of the curves to calculate parameters was done with a Python code based on [35]. A font was connected to one terminal at the distribution board, varying the tension from zero to the maximum tension of the font and measuring the current in the other terminal the IxV values were obtained. In the first months after the OPV modules were installed, the font available for the IxV measurements had a maximum voltage of 40 V. The fitting had to be done with data up to 38 V as the data were not reliable close to the maximum voltage. After the first 8 months, there was a 60 V font available and the accuracy of the IxV measurements improved and it was possible to measure J for $V = 0$.

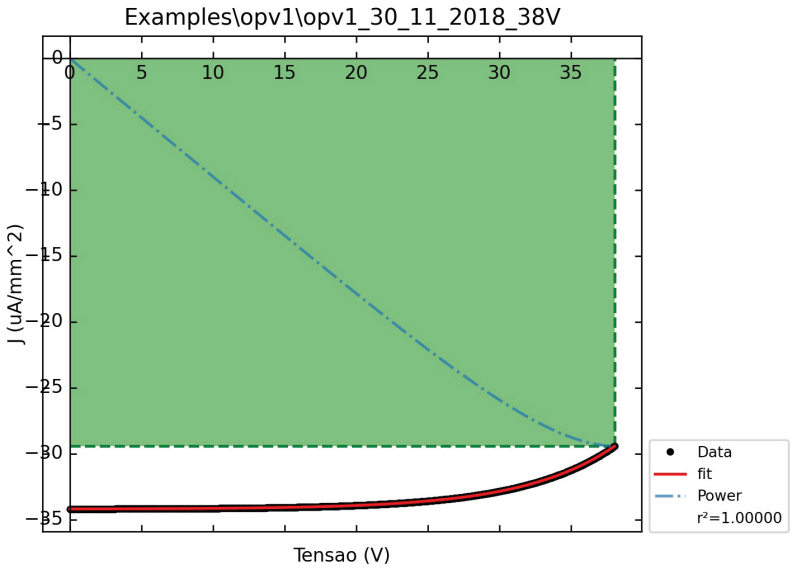

(A) JxV data and fitting, 11/30/2018

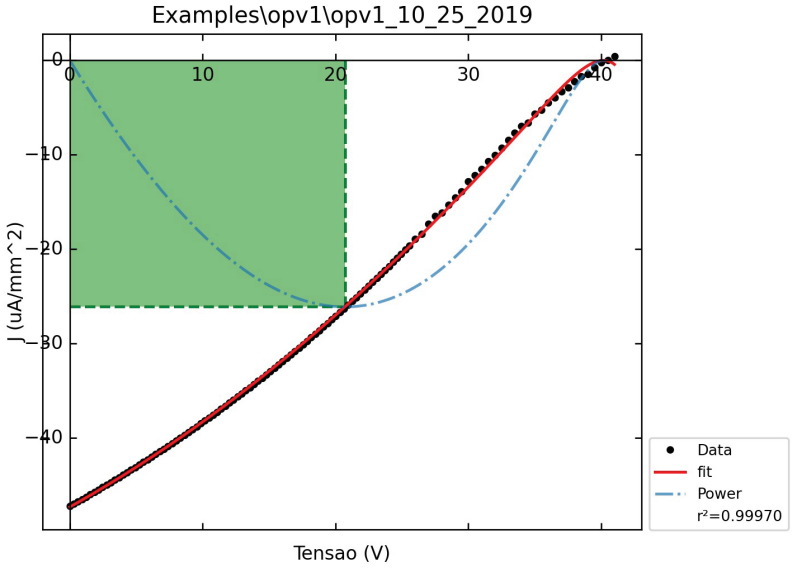

(B) JxV data and fitting, 10/25/2019

FIGURE 3.18: JxV curves and fitting, data from 2 measurements done 11 months apart

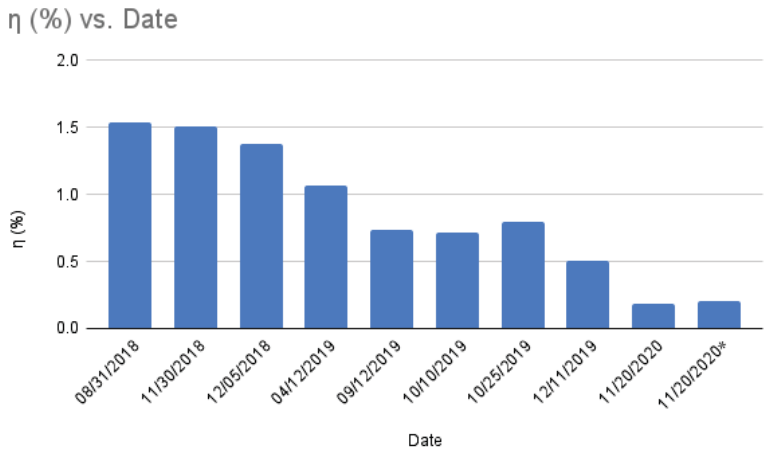

FIGURE 3.19: Efficiency of an OPV module over time

Looking at efficiency, for instance, one can get information of the performance of the PV device. In the case of the OPV modules installed on the tube-like bus station, the first measurement gave a low efficiency value as it was a cloudy day with temperature around 18^oC. Three months later, in a bright day with temperature around 28^oC, the efficiency (ν) reached 1.5%. Eight months after installation, also during a bright day with temperature around 26^oC, the efficiency was 1.0%, see Figure 3.19. At this point, the degradation of the OPV modules had to be considered as an explanation to the drop in efficiency values. Another explanation could be accumulation of soiling on the panels. Cleaning and evaluation protocols for soiling accumulation were then developed. Measurement of IxV and calculation of parameters also continued over time.

Although there was a 0.08% difference between the efficiency measured before and after cleaning the modules, soiling alone could not explain the consistent drop in efficiency values over time, see Figure 3.19 and Figure 3.21. 27 months after installation, the efficiency was almost 8 times lower than the maximum value measured (from 1.5% it dropped to 0.2%).

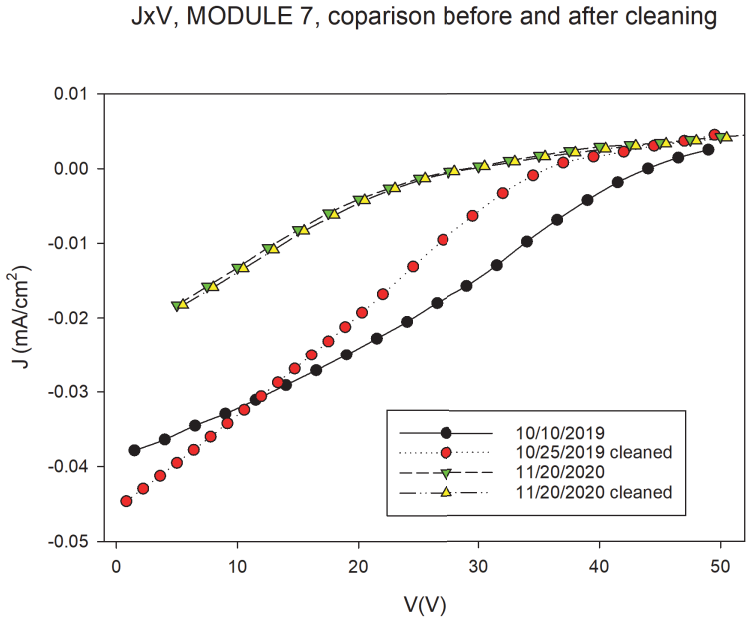

FIGURE 3.20: JxV curves measured before and after cleaning.

In order to gain knowledge on the degradation process of the OPV modules, it is important to look at other parameters presented on Table 3.2. The open circuit voltage (V_{oc}) for instance, represents the maximum voltage that a system can drawn from a device and is closely related to the efficiency of the OSC.

$$\eta = \frac{J_{sc} V_{oc} FF}{P_{in}} \tag{3.2}$$

Where J_{sc} is the short circuit current density, FF is the fill factor and P_{in} is the incident solar power. One of the factors that influences V_{oc} is the saturation current density (J_0). V_{oc} and J_0 are inversely proportional and J_0 varies exponentially with the temperature, [12]. This happens because the saturation current arises from thermally activated charge carrier injection in fullerene based OSC, [52]. V_{oc} is logarithmically related to the short circuit current density and varies linearly with the energy gap between the HOMO of the donor material and the LUMO of the acceptor material (ΔE_{DA}), see 3.3.

$$V_{oc} = \frac{n k_B T}{q} ln(\frac{J_{sc}}{J_0}) + \frac{\Delta E_{DA}}{2q} \tag{3.3}$$

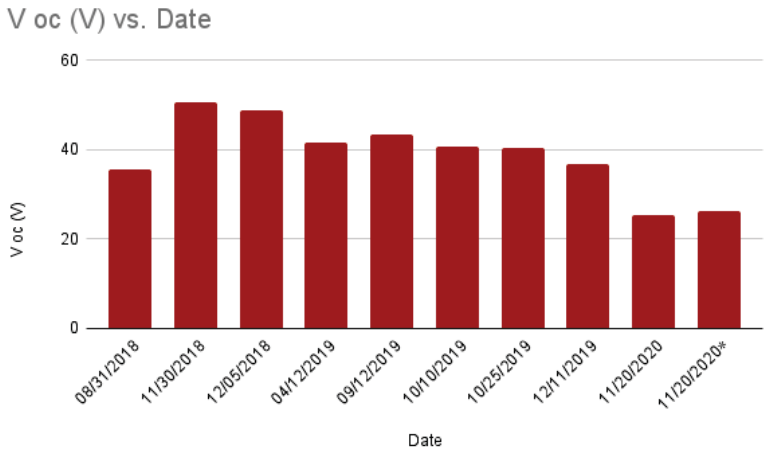

FIGURE 3.21: V_{oc} values over time, *measurement after cleaning.

In the measurements done on the OPV modules, V_{oc} decreased 48% in 27 months. As V_{oc} decreases the efficiency also decreased, see Figure 3.19 and 3.21. The fill factor (FF) that is also proportional to the efficiency decreased over time, having a maximum value of 64.77% and a minimum of 19.7%, see Table 3.2.

The short circuit current (J_{sc}) presented little change, less than one order of magnitude. As J_{sc} gives information about generation and collection of photons [37], one can infer that the degradation of the OPV modules was not due to drop in free charge carriers. As V_{oc} had a significant drop, it is likely that although the OPV modules could generate and collect carriers, the forward bias of the modules did not remain the same. The cause for that can be defects at the electrode/active layer interface or even defects in the electrodes themselves.

Another parameter that tell about the degradation of OSC is the shunt resistance (r_{sh}). When the shunt resistance is too low, the photocurrent can find an alternate path, it doesn't necessarily flow to the electrode. With this, the amount of current flowing through the OSC diminishes, reducing then the voltage. The series resistance is caused at the contact between the electrodes and the active layer and also in the interface between the electrodes

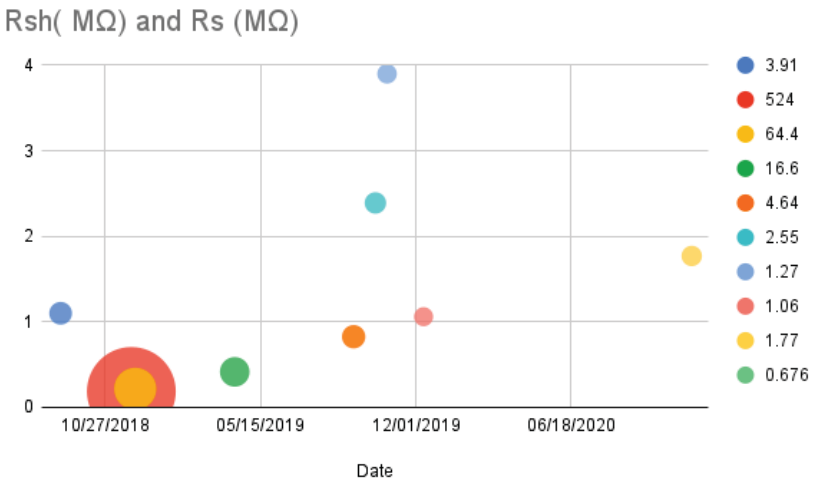

FIGURE 3.22: Diffusion plot of $r_s xtime$. The r_{sh} is represented by the bubbles.

and the base of the cell, [37]. When the series resistance (r_s) is high, because the the contact of the electrodes and the base of the cell is of poor quality, it lowers the fill factor and in some cases it can also lower the short circuit current density J_{sc}. Figure (3.22) shows a diffusion plot of r_{sh} and r_s calculated during the JxV measurements done in 27 months, data shown in Table (3.2). The values of r_{sh} decreased significantly in 27 months while the r_s oscillated. As expected, low r_s values were associated with high FF values, see Figure (3.23)

Degradation of a single module

During the 27 months when the JxV measurements took place only one panel presented a hot spot, see Figure (3.24). That particular panel was under the shadow of a tree for a few hours every day, during winter the shadow lasted longer. One and a half year after the installation it was possible to notice a spot on the panel, this panel was in a position closer to the distribution board and was part of the module identified as "module 14".

There was no significant difference in the infra red picture when comparing the spot with its surroundings, see Figure (3.25). When the operating

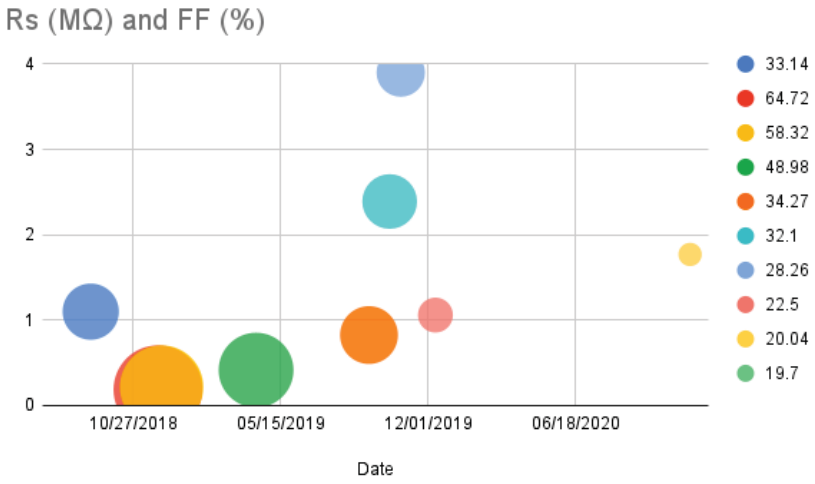

FIGURE 3.23: Diffusion plot of $r_s xtime$. The FF is represented by the bubbles.

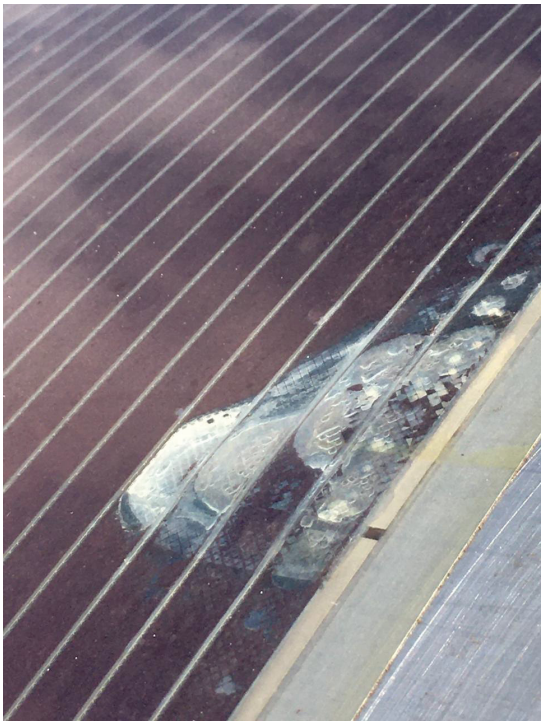

FIGURE 3.24: Hot spot on OPV module. The module was shadowed by trees part of the day.

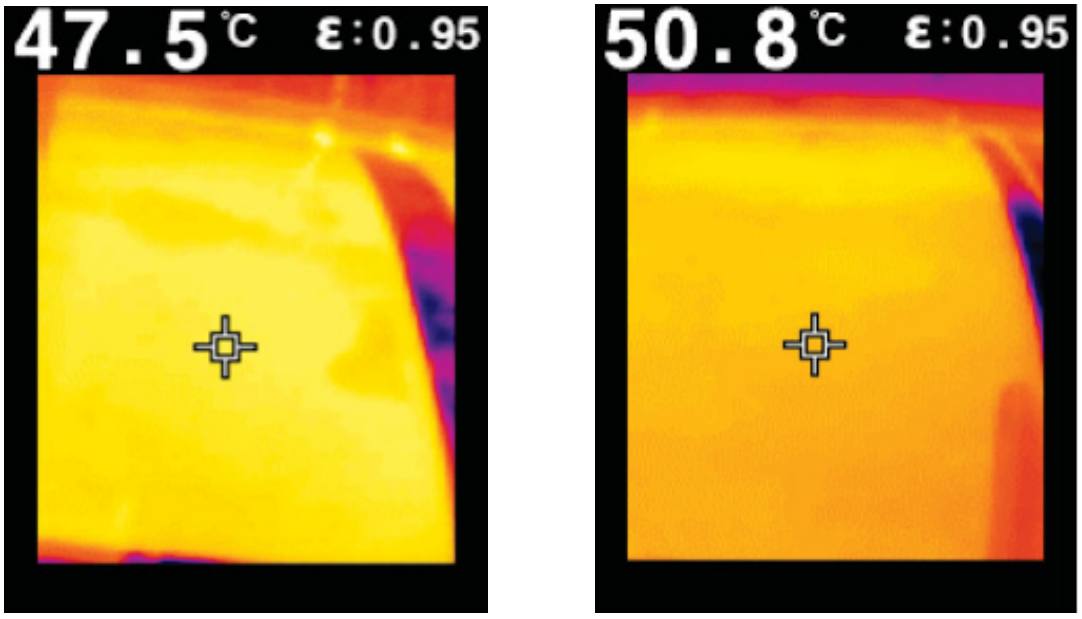

(A) IR picture of the hotspot taken in 12/26/2019

(B) IR picture of the hotspot taken in 02/27/2020

FIGURE 3.25: IR pictures of the hotspot in 2 dates 2 moths apart. No significant temperature difference observed between the spot and its surroundings.

current of a PV module is higher than the short circuit current in a shadowed cell, a hot spot occurs because the shadowed cells are forced into reverse bias dissipating power and then overheating, [1].

Although the module was still able to convert some energy, 16 months after installation all sets of OPV modules had efficiencies lower than 1%. When the second IR picture (3.25b) was taken, the efficiency of the panel was even lower, as was the efficiency of all other sets of panels, see Table (3.2). The degradation process that took place did not differ from modules without any spot to the module that presented a hot spot. The performance of the module with a spot was comparable to that of all the other modules. As can be seen in the JxV curves shown in Figure (3.26a), the degradation process went by in a pace similar to the other modules. Even in the last measurement done, it was not possible to notice more than subtle differences between the JxV curves of module 14 and the others. In Figure (3.26b) the last JxV curves measured for the module 14 (the one with a spot) and module 7, the curves

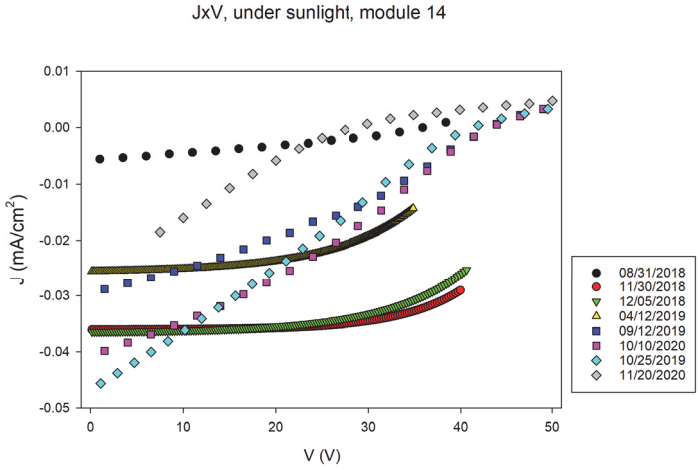

(A) JxV curves for module 14 through 27 months.

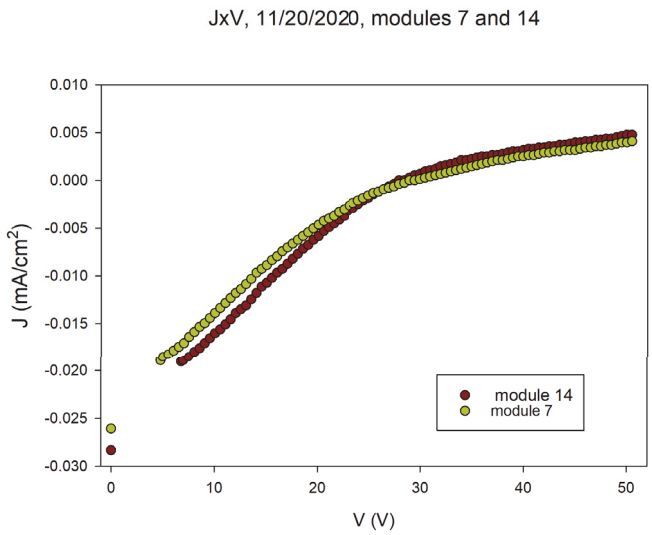

(B) JxV curves of modules 7 and 14.

FIGURE 3.26: (3.26a) JxV curves for module 14 shows a similar degradation process as observed in all the other modules.(3.26b) Comparison of the last JxV curves measured from modules 7 and 14, no significant difference is noticed.

are similar in appearance.

3.4 Soiling effect on OPV modules

The main factors a to be analysed regarding dust accumulation on solar panels are

- Chemical composition of the dust accumulated,
- Size distribution of the particles in the dust,
- Density of the dust layer deposited on the surface.

The techniques used to analyse the soiling on the OPV modules installed on the roof of the tubelike bus station were microscopy (SEM) and light transmittance. With SEM it was possible to learn about the chemical composition of the dust and also to have an idea about the size of the particles accumulated. Light transmittance can tell how much light was blocked by the dust accumulated. The protocol to collect dust on the roof of the tubelike station was to stick polyethylene terephthalate (PET) plates measuring 10x30 cm between the solar modules. Samples of the plates measuring 1x1.5 cm were then taken for microscopy and light transmittance measurements, Figure 3.27. The protocol developed for the soiling experiments is detailed in Box (3.4).

FIGURE 3.27: 10*x*30 cm PET plate sticked besides OPV module on the roof of the tublike station. 1 x 1.5 cm samples were taken from the plate each week for microscopy and transmittance measurements

Soiling exposure protocol

1. Cut PET plates in 10x30 cm pieces
2. Clean all samples with neutral detergent and water and allow them to dry.
3. Identify the samples, 1/3 of the samples will receive no coating, 1/3 of the samples will receive a hydrophobic coating and 1/3 of the samples will receive a hydrophilic coating.
4. Apply the hydrophobic coating on 1/3 of the samples with a sprinkler.
5. Spread the hydrophobic coating uniformly with a microfiber cloth.
6. Apply the hydrophilic coating on 1/3 of the samples with a sprinkler.
7. Spread the hydrophilic coating uniformly with a microfiber cloth.
8. Stick the samples with duct tape or any tape that can resist outdoors environment.

PET samples were chosen because this is the material used as a substrate and

for lamination of the OPV modules. Part of the PET samples had no previous treatment, part were treated with a hydrophobic solution (NT70) and part with a hydrophilic solution (Acquablue). Both the hydrophobic and hydrophific solutions are commercially available but their composition is not revealed by the supplier. Light transmittance measurements of the samples treated with hydrophilic solution film allowed less light to pass than the samples exposed without any treatment. Because of that response, the samples that received a hydrophilic solution film did not remain in the experiment after the first month. Prior to microscopy and transmittance measurements, part of the samples were cleaned with common neutral detergent used to clean dishes. This procedure was done to check if standard hygienization is effective to restore light transmittance.

In *Si* based solar modules, common surface treatments to mitigate soiling effects are application of hydrophobic or hydrophilic films, [39] [24]. As no reference regarding treatment of OPV modules on PET plastic substrate was found, some samples were treated with a hydrophobic film while others received a hydrophilic film. There is the possibility that other hydrophilic product could better mitigate soiling effect on OPV modules but this is yet to be tested.

3.4.1 Microscopy

The two microscopy techniques applied in the PET samples were confocal laser scanning microscopy (CLSM), scanning electron microscopy (SEM), and SEM using backscattered electrons (BSE) imaging. In imaging done using BSE, sensors detect electrons after elastic scattering with the sample, [19]. Energy dispersive X-ray spectroscopy (EDS) was used for target analysis of some samples to check their chemical composition. The protocol for the microscopy samples is described in Box (3.4.1). The techniques chosen have

been used in other works for characterization of soiling accumulated on PV modules, [9] [30] [54].

Microscopy samples protocol

1. Collect 1 x 1.5 cm samples from the PET plates that are dredged on the roof of the tubelike bus station with tweezers and a knife or scalpel.
2. Place the samples inside identified lidded containers.
3. Take the samples for microscopy.
4. The samples should be metallized with Au and fixated with a Cu tape for microscopy.
5. Identify the files with the microscopy images by field of view, date and type of the sample (exposed, cleaned before microscopy, hydrophobic, hydrophilic).

After one week of exposition it was already possible to see soiling accumulation. In Figure (3.28), it is possible to see the difference between the samples before and after cleaning.

The samples with hydrophobic and hydrophilic coatings presented different features. Hydrophobic coating prevented the sample from accumulating dust. Although the sample was not completely free of dust, it accumulated less dust than the sample without any coating, as shown in Figure (3.29a). Hydrophilic coating was not effective, the coating did not stay in an uniform layer, it probably reacted with the PET substrate. After exposure the coating formed spots on the sample, as shown in Figure (3.29b). As the hydrophilic coating could not prevent dust accumulation and could prevent photons from reaching the active layer if the OPV module received a coating with it, no other measurements were done in the samples with hydrophilic

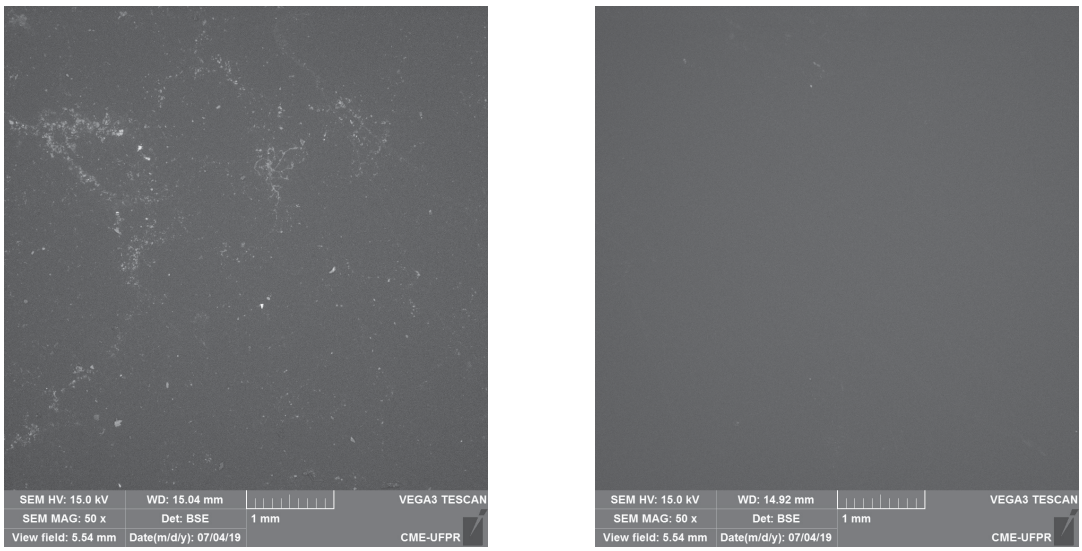

(A) Sample with dust accumulated (B) Cleaned sample

FIGURE 3.28: SEM of PET samples exposed to soiling accumulation after 1 week, (3.28a). (3.28b) Sample was cleaned before microscopy. 5.54 mm view field, BSE detection.

coating. It is worth mentioning that it is possible that other hydrophilic coating could give better results or the same coating could give better results under different weather conditions. Curitiba is a city with high humidity and this can affect the performance of the product. When applied on glass, hydrophilic coatings are effective in preventing dust accumulation [39] [24]. It is possible that the hydrophilic product used reacted with the PET substrate and for that reason its performance could not be compared with the results obtained when it is applied to glass substrate. As the goal was to reach a protocol for cleaning OPV modules encapsulated in PET within a short time, the decision taken was to move forward with the protocols that were giving the best results. Unfortunately there was no time to investigate other hydrophilic coatings or the cause that the one tried was not efficient.

In order to compare dust accumulation over time and to check for changes in different seasons, microscopy was done after 2 and 3 months of exposure. In Curitiba humidity is usually high although it can have a high gradient during the same day. Temperature can vary throughout the day, and seasons

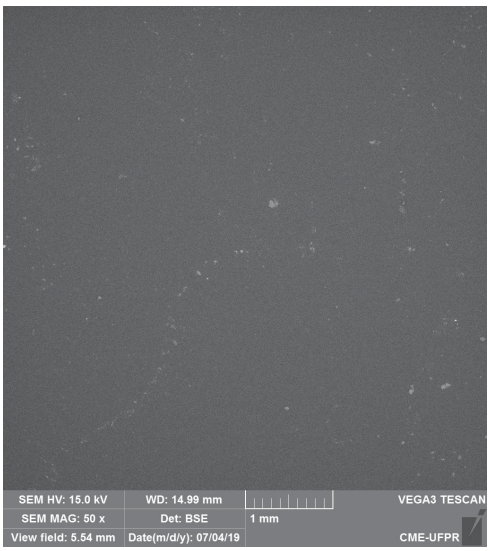

(A) Hydrophobic coating

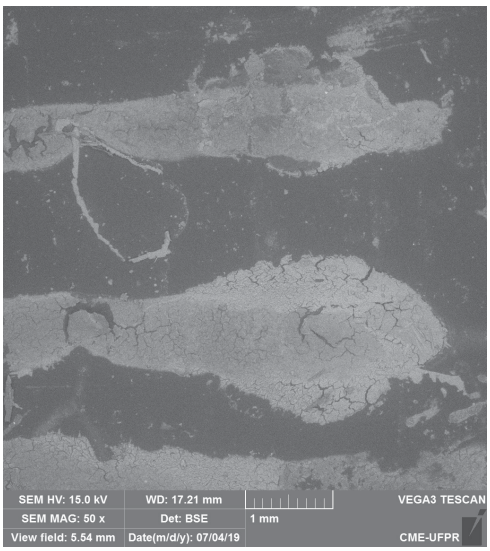

(B) Hydrophilic coating

FIGURE 3.29: SEM of PET samples with hydrophobic (3.29a) or hydrophilic (3.29b) coating exposed to soiling accumulation after 1 week. The hydrophilic coating created spots on the sample. 5.54 mm view field, BSE detection.

are defined in Curitiba, similar to other regions of the world with temperate climate. In Figure (3.30) it is possible to see humidity and temperature variation in the three months when PET samples were exposed to soiling accumulation.

Previous works have shown that high humidity helps cementation of soiling on *Si* based PV modules, [18], [30]. From the microscopy done in samples with different exposure periods we can say that the presence of larger dust spots was noticed in samples with higher exposure time and high air humidity. Samples exposed from 1 to 12 weeks are compared in Figure (3.31). For this time frame, the hydrophobic coating show a cleaner surface when compared to the samples without any treatment. Cleaning with detergent is an effective way to get rid of most soiling accumulated on PET samples.

Learning about the composition of the material accumulated on the samples helps devise a more adequate protocol for cleaning. To gain knowledge on this matter, EDS measurements were performed on all samples. As expected, he most abundant element found is carbon (*C*), since the mass of the

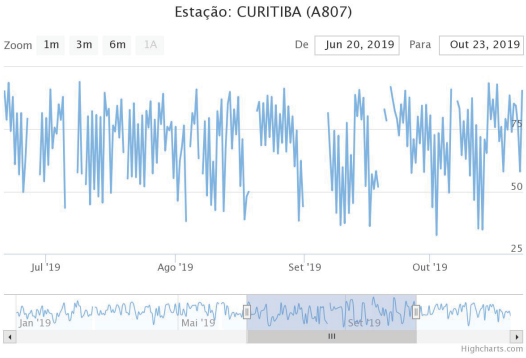

(A) Humidity in Curitiba, July to October - 2019, ©INMET, "https://tempo.inmet.gov.br/"

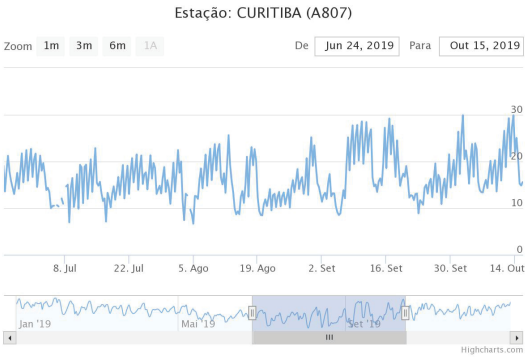

(B) Temperature in Curitiba, 07-10/2019, ©INMET, "https://tempo.inmet.gov.br/"

FIGURE 3.30: Humidity and Temperature in Curitiba, July to December - 2019

substrate PET $(C_{10}H_8O_4)_n$ has 75% of carbon. In the samples with accumulated soiling and no coating, higher amount of carbon was found. It is likely that some of the carbon found in the samples come from air pollution as the station is installed in an urban area close to an avenue with intense traffic.

All EDS measurements were done on areas of sample where material was accumulated, with a view field of $277\mu m$. The composition of the samples that were cleaned with neutral detergent before measurements were different after 1 week of exposure before cleaning than after 12 weeks of exposure before cleaning, see Figure (3.32). Each point of the sample can present a different composition as soiling does not accumulate uniformly on the PET plates. One has also to consider that the cleaning process is not as effective if the PET is exposed to the environment for a longer period before cleaning because a cementation process takes place. A thin dust layer when submitted to high humidity adheres better to the substrate surface and the dust particles

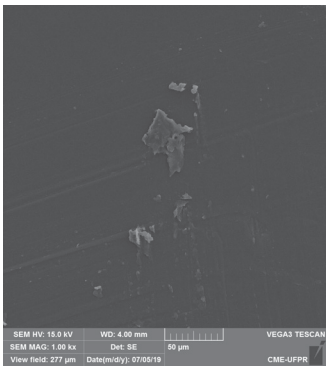

(A) SEM of a cleaned PET sample

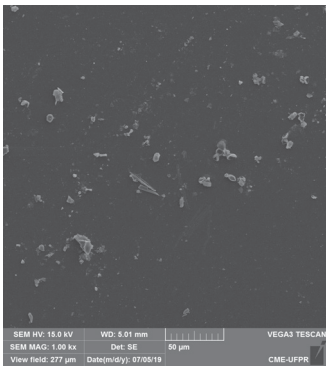

(B) SEM of a PET sample with hydrophobic coating

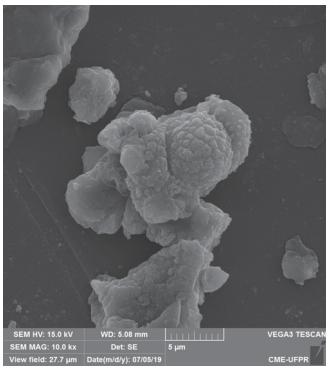

(C) SEM of a PET sample without any treatment

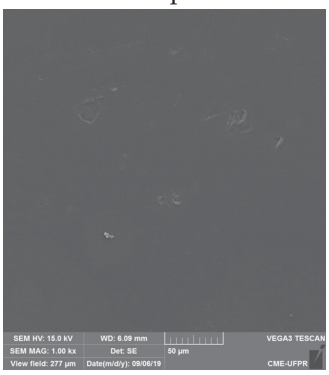

(D) SEM of a cleaned PET sample

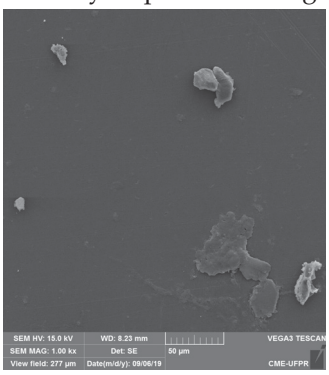

(E) SEM of a PET sample with hydrophobic coating

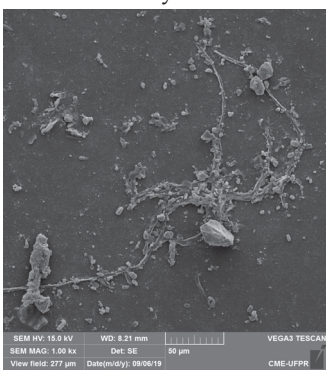

(F) SEM of a PET sample without any treatment

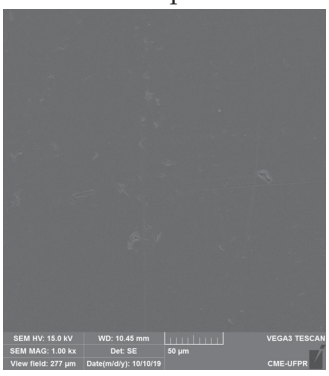

(G) SEM of a cleaned PET sample

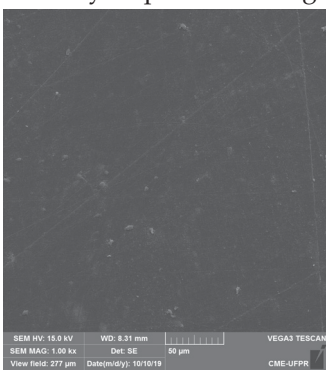

(H) SEM of a PET sample with hydrophobic coating

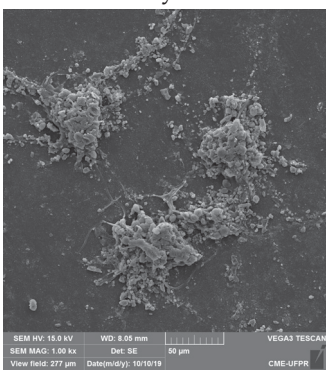

(I) SEM of a PET sample without any treatment

FIGURE 3.31: Microscopy of PET samples after 1(3.31a, 3.31c), 8 (3.31d, 3.31e, 3.31f), and 12 (3.31g, 3.31h, 3.31i) weeks of exposure. View field 277μm

also get closer together whith high humidity.

Looking at the EDS and chart of the cleaned samples, Figure 3.32, the concentration of carbon falls from 70.33% in week 1 to 55.42% in week 12 while the concentration of oxygen rises and more than 5% of silicon (Si) is present in the sample that was exposed for 12 weeks before being cleaned. It is likely that the cleaning process is not as effective if the samples are exposed for long periods before cleaning.

Samples that did not receive any treatment before EDS do not show big differences when it comes to relative concentration of carbon and oxygen, see Figure 3.33. The concentration of silicon and iron (Fe) changed, as the dust particle on the analysed after 12 weeks of exposure is likely to be a sand grain while the particle analysed after 1 week had iron and titanium (Ti). All three components (Si, Fe, Ti) are commonly found in air dust, [31].

The composition of the dust particles analysed in the samples with hydrophobic coating differ mainly in the weight relative concentration of oxygen and iron, see Figure (3.34). In the sample analysed after 1 week of exposure the iron concentration was 21.3% while in the sample exposed for 12 weeks the concentration of iron was 2.1%. The oxygen concentration jumped from 21.3% to 32.65%. The coating applied is based on hydrocarbons so it is not likely that it caused the difference in iron relative concentration. As the EDS was done for a point in the sample, the measurement is accurate for that particular point and does not tell about the average composition. EDS was also done for spectrum samples but the results were not significantly different from the punctual measurements. Because clarification on the effectiveness of the cleaning method and the efficacy of the hydrophobic coating, SEM and EDS measurements were followed by light transmittance measurements.

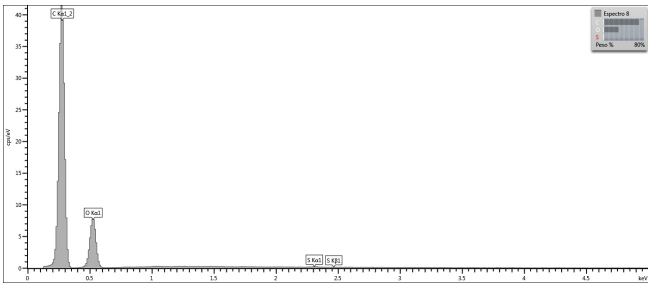

(A) Cleaned sample, 1W

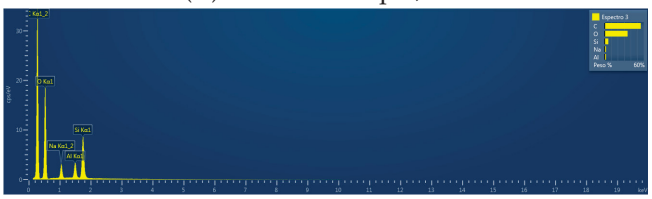

(B) Cleaned sample, 12W

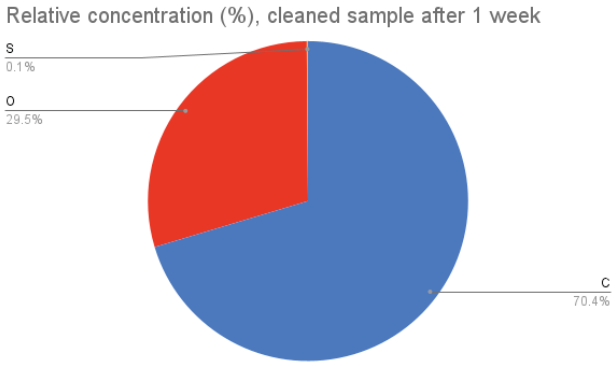

(C) Cleaned sample, components chart, 1W

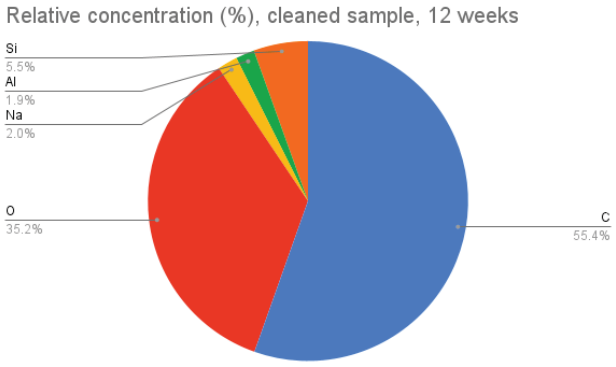

(D) Cleaned sample, components chart, 12W

FIGURE 3.32: EDS of PET samples after 1 week (3.32a) and 12 weeks (3.32b) of exposure. Charts with relative percentage of components 3.32c and 3.32d

.

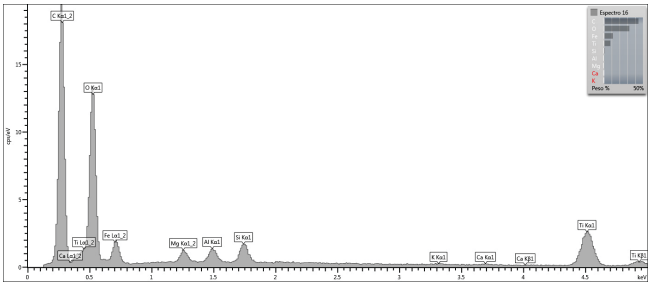

(A) Exposed sample, 1 week

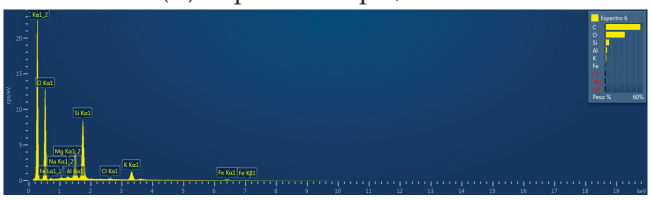

(B) Exposed sample, 12 weeks

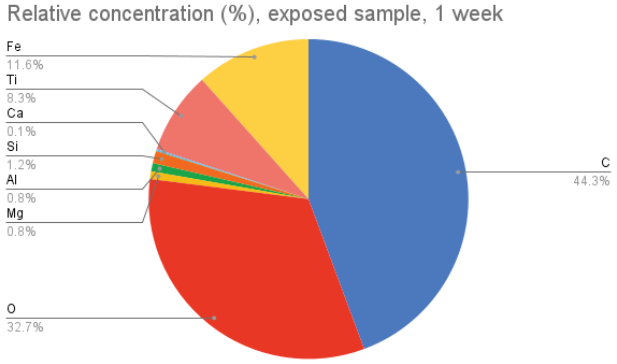

(C) Exposed sample, components chart, 1week

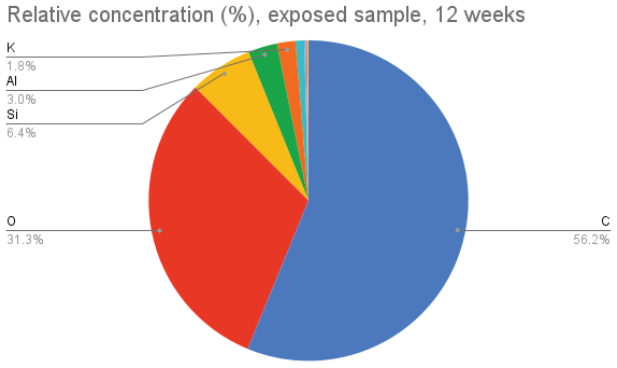

(D) Exposed sample, components chart, 12 weeks

FIGURE 3.33: EDS of PET samples after 1 week (3.33a), and 12 weeks (3.33b) of exposure.Charts with relative percentage of components, (3.33c) and (3.33d)

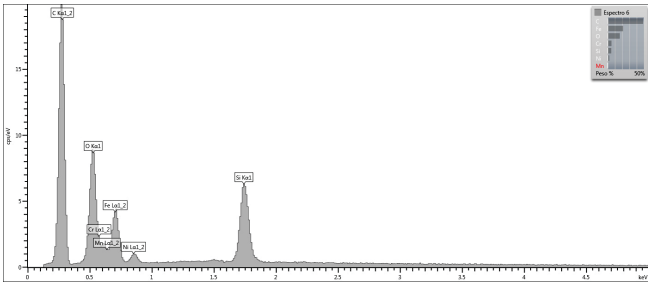

(A) Hydrophobic coating, 1 week

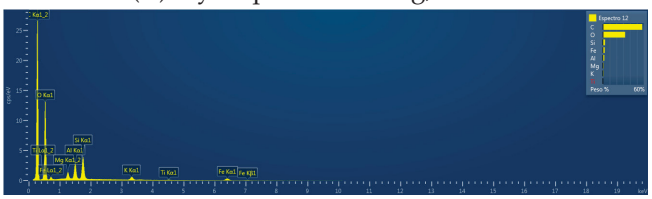

(B) Hydrophobic coating, 12 weeks

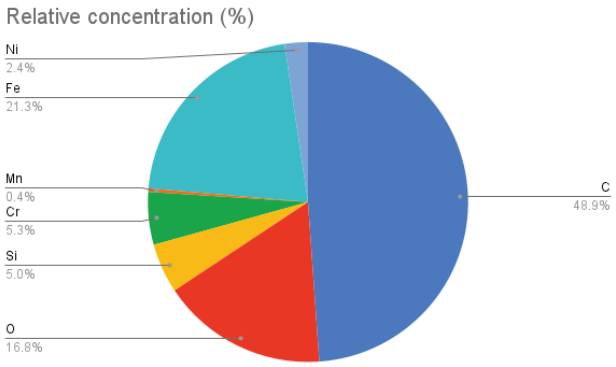

(C) Hydrophobic coating, composition chart, 1 week

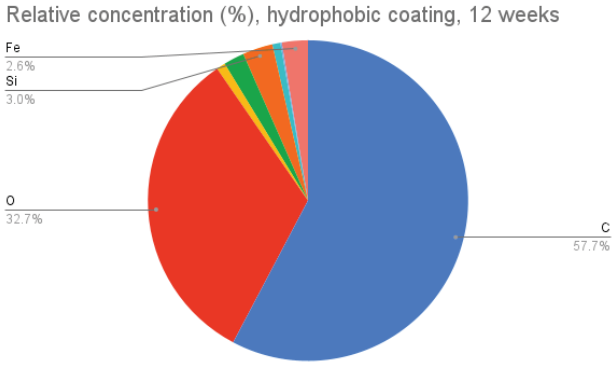

(D) Hydrophobic coating, composition chart, 12 weeks

FIGURE 3.34: EDS of PET samples after 1 week of exposure, (3.34a) and 12 weeks of exposure, (**??**) . Charts with relative percentage of components, (3.34c) and (3.34d).

3.4.2 Light Transmittance

While microscopy gives information on composition and soiling features, light transmittance shows how much light passes through a sample. As harvesting and convert sunlight energy is the main goal of PV modules, it is crucial to know how much light can pass through when soiling accumulates on the top of a module. Light transmittance measurements have been done extensively for *Si* based PV modules, [54], [39], [25].

The amount and composition of soiling can vary greatly depending on location, [3] [18] [7]. Although the surface of the PET substrate of OPV modules does not change, the measurements done in Curitiba might not apply for the same kind of OPV modules installed under different conditions. It is worth noticing that the modules were installed on the top of a curved surface, on a flat surface the amount and kind of material accumulated might differ.

Microscopy samples protocol

1. Collect two 1 x 1.5 cm samples from each type of the PET plates that are dredged on the roof of the tubelike bus station with tweezers and a knife or scalpel.
2. Place the samples inside identified lidded containers.
3. Just before light transmittance measurements, clean with water and neutral detergent one sample of each type, identify them and place in a lidded container.
4. Take at least 3 UV-Vis measurements of each sample.
5. Plot the results (Transmittance (%) x wavelength (λ).

Light transmittance measurements were performed on PET samples after 1 week, 2 weeks and 4 weeks, 8 weeks and 12 weeks after the samples were

placed on the roof of the tubelike bus station. One share of the samples was cleaned with common neutral detergent prior to measurements while other samples were not cleaned and did not receive any coating. Another share of the samples received hydrophobic coating before exposure, see Box(3.4.2). The equipment used for all light transmittance measurements was a UV-Vis Spectrophotometer Shimadzu (UV-2450), with wavelength (λ) varying from 200 to 950 nm. Cleaning with neutral detergent is an efficient way to better light transmittance of PET samples. When samples are exposed for a longer period, light transmittance does not go back to original percentage after cleaning. It is likely that cementation process takes place and adhesion of dust to PET is higher, see Figure (3.35a).

Samples that were exposed for 12 weeks had around 60% of light transmittance and around 80% after 1 week, see Figure (3.35b). This significant drop in light transmittance signalizes that soiling is an issue also for OPV modules printed on PET. Hydrophobic coating gave results similar to cleaning for the first 2 weeks, after that the coating alone was not enough to prevent light transmittance to drop, see Figure (3.35c). The comparison of the samples after 12 weeks, see Figure (3.36) shows how the hydrophobic coating allows less light to pass than the exposed samples. After 12 weeks dust starts to accumulate over the coating and blocks more light. As the use of hydrophobic coating diminished soiling accumulation over the samples in the first 2 weeks, a new protocol was conceived to check if hydrophobic coating combined with cleaning would be better to restore light transmittance than cleaning alone. The new protocol added a light transmittance measurement after cleaning the samples that received a hydrophobic coating. Cleaning the PET samples that received hydrophobic coating prior to exposure restored light transmittance to the same level as samples that received no treatment

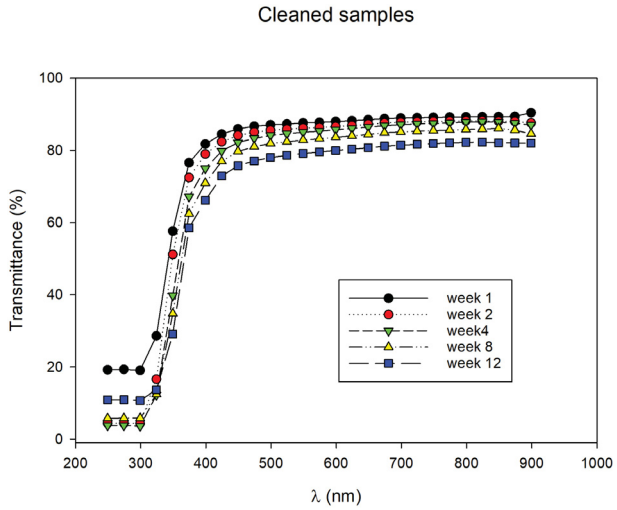

(A) Cleaned samples, 1-12 weeks

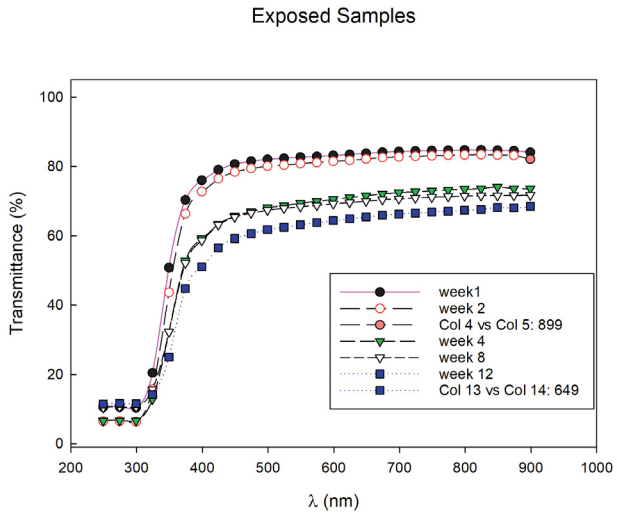

(B) Exposed samples, 1-12 weeks

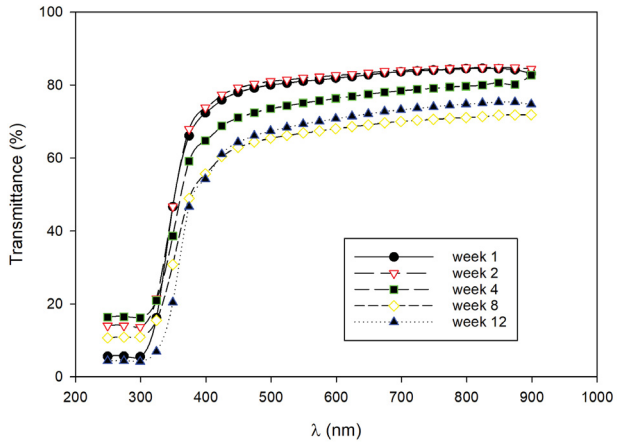

(C) Hydrophobic coating, 1-12 weeks

FIGURE 3.35: Light transmittance measurements of samples exposed for 1-12 weeks, 3.35a, 3.35b, 3.35c. Higher difference in light transmittance is noticed in 3.35b.

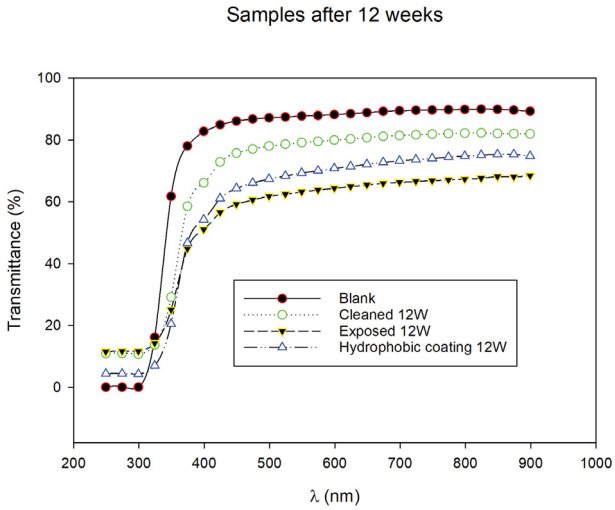

FIGURE 3.36: All samples after 12 weeks. cleaned samples have a small change in light transmittance while exposed samples show a significant change.

and were cleaned before measurements, see Figure (3.37). As the hydrophobic coating prevented soiling accumulation in the first 2 weeks, the coating is effective to allow for sparser cleaning schedule.

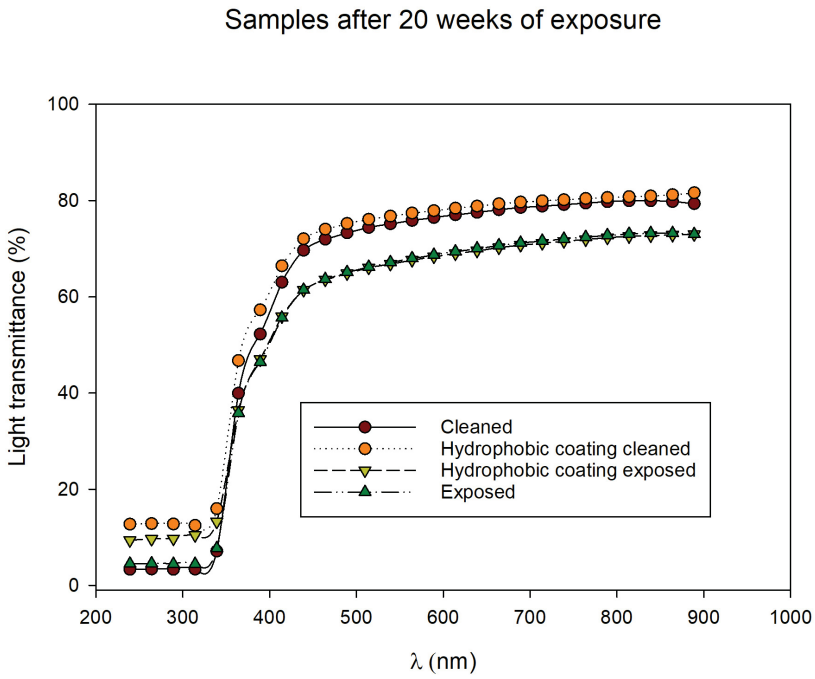

(A) Samples after 20 weeks of exposure

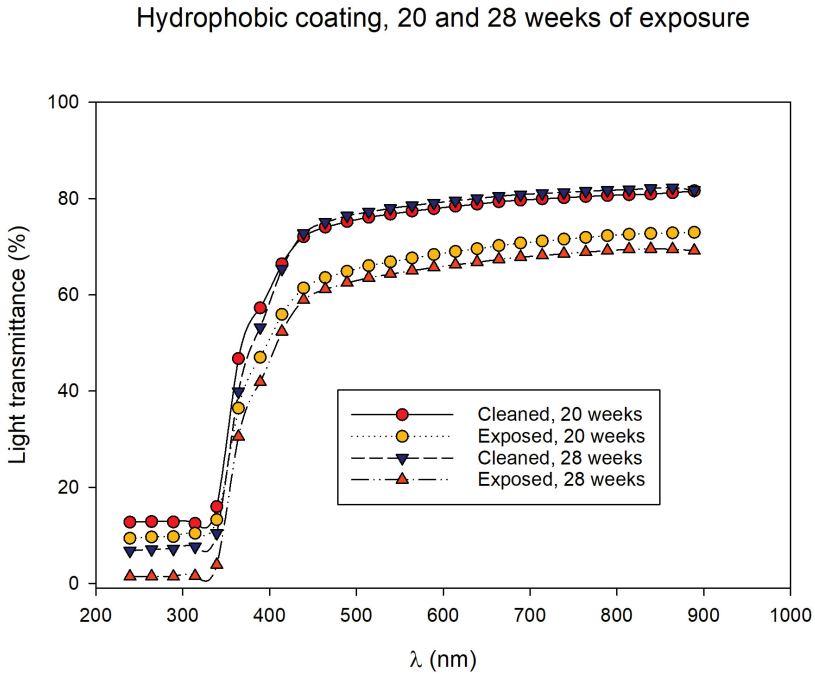

(B) Hydrophobic coating cleaned and exposed samples, 20 and 28 weeks

FIGURE 3.37: Light transmittance after 20 weeks of exposure, 3.37a, samples with and without hydrophobic coating before and after cleaning. Samples with hydrophobic coating after 20 and 28 weeks before and after cleaning, 3.37b

Chapter 4

Conclusion

The main goal of this thesis was to evaluate commercially available OSC modules under real use conditions. The tubelike bus station that is a symbol of the city of Curitiba was the piece of urban furniture chosen to test the use of OSC. What is possible to conclude after elaborating protocols and following them for over 2 years is

1. The commercially available OSC evaluated were able to hold their efficiency for around 6 months, after that period degradation of the modules caused them to progressive loss in efficiency.

2. Possible causes for efficiency loos are defects in the active layer/electrode interface, defects in the electrodes and/or issues related to the connection between the 64 cells that are connected in series in each set of OPV modules. Those defects could have been caused by a combination of high temperatures at the top of the stainless steel roof, high humidity and many days with high irradiation.

3. Concerning accumulation of soiling on the top of the OPV modules, a cleaning protocol was developed. The modules should receive a hydrophobic coating prior to installation. Every week the OPV panels should be cleaned with common neutral detergent to avoid light transmittance loss.

4. The main question to be answered regards the use of OSC in urban furniture. Although degradation of the modules is an issue, the fact that the panels can adapt to almost any shape of furniture is an advantage. In the case of original designs, such as the tubelike bus station, OSC are a way of generating sustainable energy without compromising the design. As the environmental cost of production of OSC is lower than any other solar technology available, [28], public investment in uses for this technology will help lower the cost of production and increase society awareness.

Chapter 5

Future work

A few questions regarding the evaluation of commercially available OSC remain to be answered.

- Only one brand of OSC was tested in this thesis. To have a clear picture of the performance of the technology in general another project involving OSC from different suppliers should be developed.
- The cause for the degradation of the OPV modules remain unknown. Find the cause and ways to mitigate degradation of the modules is the next step to improve the technology.
- This thesis presents the first study on soiling effect on thin film based solar modules while the bibliography on soiling effect on *Si* based modules is vast. Although some protocols can be derived from that literature, specific protocols for OPV modules should be done.

Bibliography

[1] Shifeng Deng et al. "Research on hot spot risk for high-efficiency solar module". In: *Energy Procedia* 130 (2017), pp. 77–86. DOI: 10.1016/j.egypro.2017.09.399.

[2] Salima Alem, Remi de Bettignies, and Jean-Michel Nunzi. "Efficient polymer-based interpenetrated network photovoltaic cells." In: *Appl. Phys. Lett.* 84 (2004), pp. 2178–2180. DOI: 10.1063/1.1669065.

[3] Thamer Alquthami and Karim Menoufi. "Soiling of Photovoltaic Modules: Comparing between Two Distinct Locations within the Framework of Developing the Photovoltaic Soiling Index (PVSI)". In: 11(17) (2019), p. 4697.

[4] Various authors. "SETO 2020 peer review report". In: *Solar Energies Technology Office* (2020), pp. 7–10. URL: https://www.energy.gov/eere/solar/downloads/seto-2020-peer-review-report.

[5] R. Berger, A. L. Domanskia, and Weber S.A.L. "Electrical characterization of organic solar cell materials based on scanning force microscopy". In: *European Polymer Journal* 49(8) (2013), pp. 1907–1915. DOI: 10.1016/j.eurpolymj.2013.03.005.

[6] SCarla D. Canestraro et al. "Carbon nanotubes based nanocomposites for photocurrent improvement". In: *AApplied Surface Science* 252 (15) (2006), pp. 5575–5578. URL: https://doi.org/10.1016/j.apsusc.2005.12.139.

[7] Yusuf N. Chanchangi et al. "An analytical indoor experimental study on the effect of soiling on PV, focusing on dust properties and PV surface material". In: *Solar Energy* 203 (2020), pp. 46–68. DOI: 10.1016/j.solener.2020.03.089.

[8] Ricardo Conceição et al. "Organic Soiling: The Role of Pollen in PV Module Performance Degradation". In: *Energies* 11.2 (2018), p. 294. DOI: 10.3390/en11020294.

[9] Rached Dhaouadi et al. "A characterization study for the properties of dust particles collected on photovoltaic (PV) panels in Sharjah, United Arab Emirates". In: *Renewable Energy* 171 (2021), pp. 133–140. DOI: 10.1016/j.renene.2021.02.083.

[10] Nutifafa Y. Doumon et al. "Photostability of Fullerene and Non-Fullerene Polymer Solar Cells: The Role of the Acceptor". In: *ACS Appl. Mater. Interfaces* 11(8) (2019), pp. 8310–8318. DOI: 10.1021/acsami.8b20493.

[11] Mohammad S. El-Shobokshy and Fahmy M. Hussein. "Degradation of photovoltaic cell performance due to dust deposition on to its surface". In: *Renewable Energy* 3.6 (1993), pp. 585–590. DOI: 10.1016/0960-1481(93)90064-N.

[12] Naveen Kumar Elumalai and Ashraf Uddin. "Open circuit voltage of organic solar cells: an in-depth review". In: *Energy Environ. Sci.* 9 (2016), pp. 391–410. DOI: 10.1039/C5EE02871J.

[13] Camara de comercialização de energia elétrica. *Resultados de leilões*. URL: "https://www.ccee.org".

[14] K. Feron et al. "Organic solar cells: understanding the role of Förster resonance energy transfer." In: *International journal of molecular sciences* 13 (2012), 17019–17047. URL: https://doi.org/10.3390/ijms131217019.

[15] Fraunhofer Institute for Solar Energy Systems. *"Photovoltaics report"*. acessed:02.07.2021. URL: https://www.ise.fraunhofer.de/content/dam/ise/de/documents/publications/studies/Photovoltaics-Report.pdf.

[16] Yunier Garcia-Basabe et al. "The effect of thermal annealing in the charge transfer dynamics of a donor-acceptor copolymer and fullerene: F8T2 and F8T2:PCBM". In: *Phys. Chem. Chem. Phys.* 17 (Mar. 2015). DOI: 10.1039/C5CP01285F.

[17] Yunier Garcia-Basabe et al. "Ultrafast interface charge transfer dynamics on P3HT/MWCNT nanocomposites probed by resonant Auger spectroscopy". In: *RSC Advances* 8 (2018), pp. 26416–26422. URL: https://doi.org/10.1039/C8RA04629H.

[18] S. Ghazi, A. Sayigh, and K. Ip. "Dust effect on flat surfaces – A review paper". In: *Renewable and Sustainable Energy Reviews* 33 (2014), pp. 742–751. DOI: 10.1016/j.rser.2014.02.016.

[19] J. Goldstein et al. *Scanning Electron Microscopy and X-Ray Microanalysis. A Text for Biologists, Materials Scientists, and Geologists*. New York: Plenum Press, 1981. ISBN: 978-0-306-40768-0.

[20] Alan J. Heeger. "25th Anniversary Article: Bulk Heterojunction Solar Cells: Understanding the Mechanism of Operation". In: *Advanced Materials* 26 (2013), pp. 10–28. URL: https://doi.org/10.1002/adma.201304373.

[21] Ken Ishikawa James H.Dickerson Huanqi Cao Weidong Hea Yiwu Mao Xiao Lin and Wayne P.Hess. "Recent progress in degradation and stabilization of organic solar cells". In: *Journal of Power Sources* 264 (2014), pp. 168–183. DOI: 10.1016/j.jpowsour.2014.04.080.

[22] Olle Iganäs. "Organic Photovoltaics over Three Decades". In: *Advanced Materials* 30 (2018), pp. 935–964. URL: https://doi.org/10.1002/adma.201800388.

[23] International Energy Agency. *"IEA PV report 2020," Feb. 02, 2021*. URL: https://www.iea.org.

[24] Magnum Augusto Moraes Lopes de Jesus et al. "Anti-soiling coatings for solar cell cover glass: Climate and surface properties influence". In: *Solar Energy Materials and Solar Cells* 185 (2018), pp. 517–523. DOI: 10.1016/j.solmat.2018.05.036.

[25] Lawrence L. Kazmerski et al. "Fundamental Studies of Adhesion of Dust to PV Module Surfaces: Chemical and Physical Relationships at the Microscale". In: *IEEE Journal of Photovoltaics* 6.3 (2016), pp. 719–729. DOI: 10.1109/JPHOTOV.2016.2528409.

[26] M. Koehler et al. "The current-voltage characteristics of polymer/C60 diodes in the dark: A direct way to assess photovoltaic devices efficiency parameters". In: *Applied Physics Letters* 103(3) (2013), p. 033304. DOI: 10.1063/1.4813759.

[27] G. Li, R. Zhu, and Y. Yang. "Polymer solar cells." In: *Nature Photon.* 6 (2012), pp. 153–161. DOI: 10.1038/nphoton.2012.11.

[28] Sebastien Lizin et al. "Life cycle analyses of organic photovoltaics: a review". In: *Energy Environ. Sci.* 6 (2013), pp. 3136–3149. DOI: 10.1039/C3EE42653J.

[29] L. Lu, M. Kelly, and W. et al. You. "Status and prospects for ternary organic photovoltaics." In: *Nature Photon.* 9 (2015), pp. 491–500. DOI: 10.1038/nphoton.2015.128.

[30] Mohammad Reza Magham et al. "Power loss due to soiling on solar panel: A review". In: *Renewable and Sustainable Energy Reviews* 59 (2016), pp. 1307–1316. DOI: 10.1016/j.rser.2016.01.044.

[31] Yigiterhan O. Elnaiem A.E. et al. Mahfouz M.M. "Elemental compositions of particulate matter retained on air condition unit's filters at Greater Doha, Qatar." In: *Environ Geochem Health* 41 (2019), 2533–2548. DOI: 10.1007/s10653-019-00304-8.

[32] Luana Cristina Wouk de MenezesLuana Cristina Wouk de Menezes et al. "Charge Transfer Dynamics and Device Performance of Environmentally Friendly Processed Nonfullerene Organic Solar Cells". In: *ACS Appl. Energy Mater.* 9 (2018), pp. 4776–4785. URL: https://doi.org/10.1021/acsaem.8b00884.

[33] S. Matthew Menke et al. "Understanding Energy Loss in Organic Solar Cells: Toward a New Efficiency Regime." In: *Joule* 2 (2018), pp. 25–35. URL: https://www.cell.com/joule/pdf/S2542-4351(17)30094-6.pdf.

[34] Frederik C. Krebs Mikkel Jørgensen. "Degradation of Polymer-Based OPV". In: *Stability and Degradation of Organic and Polymer Solar Cells* (2012), pp. 143–162. DOI: 10.1002/9781119942436.ch6.

[35] André Moliton and Jean-Michel Nunzi. "How to model the behaviour of organic photovoltaic cells". In: *Polymer International* 55 (2006), pp. 583–600. URL: https://doi.org/10.1002/pi.2038.

[36] National Renewable Energy Laboratory. *"Best Research-Cell Efficiency Chart"*. acessed:02.07.2021. URL: https://www.nrel.gov/pv/cell-efficiency.html.

[37] Jenny Nelson. *The Physics of Solar Cells*. 57, Shelton Street, London: Imperial College Press, 2003.

[38] Jonas Rabinovitch and Josef Leitman. "Urban Planning in Curitiba." In: *Scientific American* 274 ().

[39] Małgorzata Rudnicka and Ewa Klugmann-Radziemska. "Soiling Effect Mitigation Obtained by Applying Transparent Thin-Films on Solar Panels: Comparison of Different Types of Coatings". In: *Materials* 14.4 (2021), p. 964. DOI: 10.3390/ma14040964.

[40] Mohammad S., El-Shobokshy, and Fahmy M. Hussein. "Effect of dust with different physical properties on the performance of photovoltaic cells". In: *Solar Energy* 51.6 (1993), pp. 505–511. DOI: 10.1016/0038-092X(93)90135-B.

[41] Travis Sarvera, Ali Al-Qaraghuli, and Lawrence L.Kazmerski. "A comprehensive review of the impact of dust on the use of solar energy: History, investigations, results, literature, and mitigation approaches". In: *Renewable and Sustainable Energy Reviews* 22 (2013), pp. 698–733. DOI: 10.1016/j.rser.2012.12.065.

[42] M.C. Scharber et al. "Design Rules for Donors in Bulk-Heterojunction Solar Cells—Towards 10% Energy-Conversion Efficiency". In: *Advanced Materials* 18 (2006), 789–794. URL: https://doi.org/10.1002/adma.200501717.

[43] Lin Simpson. "Addressing Soiling: From Interface Chemistry to Practicality". In: *Golden, CO: National Renewable Energy Laboratory* NREL/TP-5K00-72853 (2020). URL: "https://www.nrel.gov/docs/fy20osti/72853.pdf".

[44] Eduardo von Sperling. "Hydropower in Brazil: Overview of Positive and Negative Environmental Aspects". In: *Energy Procedia* 18 (2012), pp. 110–118.

[45] Roar Søndergaard et al. "Roll-to-roll fabrication of polymer solar cells". In: *Materials Today* 15.1 (2012), pp. 36–49. ISSN: 1369-7021. DOI: https://doi.org/10.1016/S1369-7021(12)70019-6. URL: https://www.sciencedirect.com/science/article/pii/S1369702112700196.

[46] Anna Gabriella Tempesta et al. "Organic Photovoltaic Solar Panels Applied to a Tubelike bus Station". In: *Brazilian Physics Journal, submitted* (2021).

[47] Various authors. *"Solar PV Battery Manual. USAID/CLEAN", 2018*. accessed: 09.01.2020. URL: http://ces-ltd.in/wp-content/uploads/2018/12/Manual_0410.pdf.

[48] Various authors, International Energy Agency. *"Data explorer, Brazil, hydro. IEA reports", Feb. 02, 2021*. URL: https://www.iea.org/articles/renewables-2020-data-explorer.

[49] Various authors, United Nations. *"Affordable and clean energy", Feb. 02, 2021*. URL: https://sdgs.un.org/goals/goal7.

[50] Various authors, United Nations. *"Sustainable Development Goals", Feb. 02, 2021*. URL: https://sdgs.un.org/goals.

[51] Alan J. Heeger Wei Lin Leong Sarah Cowan. "Differential Resistance Analysis of Charge Carrier Losses in Organic Bulk Heterojunction Solar Cells: Observing the Transition from Bimolecular to Trap-Assisted Recombination and Quantifying the Order of Recombination". In: *Advanced Energy Materials* 4 (2011), pp. 517–522. DOI: 10.1002/aenm.201100196.

[52] Asha Sharma William J. Potscavage Jr. and Bernard Kippelen. "Critical Interfaces in Organic Solar Cells and Their Influence on the Open-Circuit Voltage". In: *Acc. Chem. Res.* 42.11 (2009), pp. 1758–1767. DOI: 10.1021/ar900139v.

[53] Natasha A.D. Yamamoto et al. "Charge transport model for photovoltaic devices based on printed polymer: Fullerene nanoparticles". In: *Solar Energy Materials Solar Cells* 141 (2015), pp. 171–177. DOI: 10.1016/j.solmat.2015.05.034.

[54] B. Yilbas, H. Ali, and M. et al. Khaled. "Influence of dust and mud on the optical, chemical and mechanical properties of a pv protective glass." In: *Sci Rep* 5 (2015), p. 15883. DOI: 10.1038/srep15833.

[55] M. Zhang, L. Zhu, and G. et al. Zhou. "Single-layered organic photovoltaics with double cascading charge transport pathways: 18% efficiencies." In: *Nature Commun.* 12(309) (2021). DOI: 10.1038/s41467-020-20580-8.

[56] Song Zhang et al. "The Critical Role of Electron-Donating Thiophene Groups on the Mechanical and Thermal Properties of Donor–Acceptor Semiconducting Polymers". In: *Advanced Electronic Materials* 5 (2019), pp. 1800–1899. URL: https://doi.org/10.1002/aelm.201800899.

[57] Tan H.S. Guo X. et al. Zhang J. "Material insights and challenges for non-fullerene organic solar cells based on small molecular acceptors". In: *Nat. Energy* 3 (2018), pp. 720–731. DOI: 10.1038/s41560-018-0181-5.

Appendix A

Article 1

ORGANIC PHOTOVOLTAIC SOLAR PANELS (OPV) APPLIED TO A TUBE-LIKE BUS STATION

ORGANIC PHOTOVOLTAIC SOLAR PANELS (OPV) APPLIED TO A TUBELIKE BUS STATION

Anna Gabriella Tempesta[1*], Luiz Carlos Mariano[2], Kaike Rosivan Maia Pacheco[2], Talitha Ramos Canabarra dos Santos[2], Maria Luiza Miranda Rocco[3], Lucimara Stolz Roman[1,2]

1 Graduate program on Engineering and Material Science, Federal University of Parana, Caixa Postal 19011, CEP: 81531-980, Curitiba, PR

2 Physics Department, Federal University of Parana, Caixa Postal 19044, CEP: 81531-980, Curitiba, PR

3 Institute of Chemistry, Federal University of Rio de Janeiro, CEP: 21941-909, Rio de Janeiro, RJ, Brazil

*anna.tempesta@ufpr.br, corresponding author

Abstract:

Organic solar panels (OPV) are an alternative to silicon (Si) based solar panels as they can be applied to flexible substrates such as polyethylene terephthalate (PET). Although the efficiency of organic solar panels is lower than that of Si-based ones, their potential for use in urban furniture is big because of their light weight and for the fact that they can be applied to non-even surfaces. In this paper, we report the characteristics of a polymer-fullerene organic photovoltaic modules and their use on the metal roof of a tubular bus station, a typical construction from the city of Curitiba. The solar panels installed were commercial modules obtained by roll-to-roll printing at large area that are nowadays are available to the market. We have used 28 panels and based on that we develop a low-cost electrical project for the bus station. We investigate the current voltage characteristics of the selected panels and discuss their efficiency over half year project. The physico-chemical characterization of the OPV films were obtained by X-Ray photoelectron spectroscopy endorsing the high-quality blend film obtained by slot die printing used in our project.

Keywords: Organic solar panels, OPV, solar panels for urban furniture.

Appendix B

Article 2

Organic photovoltaic panels for bus rapid transit stations in Curitiba – a viability study

Organic photovoltaic panels for bus rapid transit stations in Curitiba – a viability study

Anna Gabriella Tempesta[1], Luiz Carlos Mariano[1], Kaike R. M. Pacheco[1], Talitha R. C. dos Santos[1], Fabiana Brito and Lucimara Stolz Roman[1]

[1] Grupo de Dispositivos Nanoestruturados (DiNE), Universidade Federal do Paraná (UFPR,) Curitiba -Brazil

Abstract

Curitiba is the capital city of Parana State in Brazil. The city is famous for its urban plan and Bus Rapid Transit (BRT) system. The cylindric design of the bus stations, known as tubelike stations, in Curitiba's BRT system, is unique and considered a symbol of the city. Recently these bus stations have been criticized for lacking thermal comfort and for their high-power consumption (around 18 kWh/day). Organic Photovoltaic (OPV) solar panels printed on flexible polyethylene terephthalate (PET) substrate can be a solution to locally generate power without altering the unique design of the stations. The energy provided by OPV panels should cover at least 60% of that demand to be economically viable. In this work we analyzed efficiency, reliability and resilience of OPV panels installed on the top of a tubelike station for 11 months. Performance related parameters (JxV curves, J_{SC}, V_{OC}, irradiance) were measured and a methodology to test soiling effects on the OPV panels was designed. Because there are not many publications on soiling effects on OPV panels the methodology used in this work was adapted from methodologies described in works on soiling effects on Si based PV modules.

Keywords: OPV, urban furniture, flexible solar panels, efficiency analysis, soiling effects on PV modules.

1. Introduction

Bus rapid transit (BRT) is the main public transportation system in Curitiba. BRT stations in Curitiba were revamped back in 1991 and since then became a symbol of the city (Leitman and Rabinovich, 1996). On more than one occasion interventions to the iconic tubelike bus stations were proposed and were not accepted because they added major changes to the original design of the stations.

The average energy consumption of a standard tubelike station is, according to the Urban Administration Office (URBS) of Curitiba, 180 kWh per month. URBS will only consider installing OPV panels on BRT stations if the panels can generate at least 60% of the power demand of each station. Analysis of energy efficiency, environmental cost and adaptation of solar cells to a standard tubelike station will help local administration to decide on the use of OPV panels for BRT stations and other urban furniture.

In this work we report the performance of Organic Photovoltaic (OPV) panels that were installed in a test tubelike station. URBS donated the station that was installed inside Universidade Federal do Parana (UFPR) campus that is destined to research and development of technologies that might be later reproduced in other tubelike stations in Curitiba.

Although OPV based cells have been studied for over 30 years (Inganas, 2018), the industrial production of the panels only happened a few years ago. OPV panels enable better architectural integration and also have the advantage of having a production with less environmental impact than the production of Si based solar panels (Hengevoss et al, 2016). Production of OPV panels should soon have even less environmental impact with the use of green solvents that have been recently researched (Wouk de Menezes et. al, 2018).

The lack of viability studies on market ready OPV panels in climate conditions similar to those in Curitiba motivated us to design a comprehensive set of measurements that evaluate efficiency, reliability and

doi:10.18086/swc.2019.15.04 Available at http://proceedings.ises.org

resilience of the panels in Curitiba. As OPV panels can be printed on flexible substrates like PET they have potential to be used on windows and urban furniture.

The OPV panels studied in this work were produced by CSEM Brasil using roll to roll technique (Hosel et al, 2012) and are available to the market. The panels were installed on the top of the test tubelike station (Figure 1).

Figure 1: Test tubelike station at UFPR campus. CSEM OPV panels are installed on the top of the station.

The main difference between organic and Si-based solar cells is in the semiconductor layer. In organic cells, this layer uses organic compounds (usually C60 and derivatives) as electron receptors and an electron donor polymer, such as P3HT. The organic solar panels installed on the top of the test tubelike station were produced by CSEM / SUNEW.

In this viability study we periodically measured open circuit potential (V_{OC}) and short circuit current (I_{SC}) *of* 14 sets of 2 solar panels to evaluate their efficiency in different seasons. Efficiency measurements usually done in a lab environment on 10 *cm* x 10 *cm* cells as described by Canestraro 2007 and Cava 2013 were adapted to measure the efficiency of the OPV panels. The measurements made by Krebs, F.C. et al in 2014 were also a reference for our measurement protocol.

Figure 2 shows how the panels are disposed on the top of the test tubelike station. We also present an experimental setup to test how soilingt affects efficiency of OPV panels and to characterize the dust that adheres to the panels in Curitiba. Previous works on soiling that guided our choice of experimental setup were reviewed in Kazmerski et al, 2013. Although none of the soiling studies presented by this review were done for OPV panels it was possible to adapt the protocols to our setup.

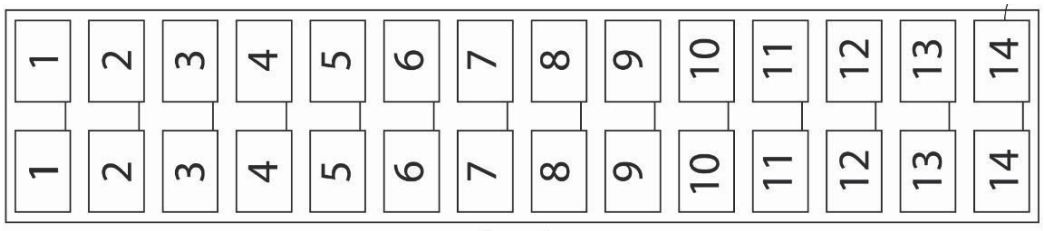

Figure 2: Arrangement of panels on top of the bus shelter.

2. Materials and Methods

2.1 Solar Panels

The test tubelike bus shelter was installed inside the university campus between a parking lot and a campus road. 28 OPV solar panels printed on polyethylene terephthalate (PET) were installed over the top of a cylindrical bus shelter, see Figure 2. The panels were connected in series in sets of 2. The 14 sets of panels were then connected in parallel. 2 sets of panels are under a tree shadow part of the day. The panels are connected to an energy monitoring system that allows voltage readings of the 14 sets of panels separately.

2.2 Sample preparation for microscopy and transmittance measurements

PET samples measuring 10 cm x 30 cm were taped on the top of the bus shelter between OPV panels. Part of the samples received a film of a hydrophobic solution (NT70) and part of the samples didn't receive any treatment. Prior to transmittance measurements and microscopy, part of the samples were cleaned with common neutral detergent. This procedure was done to check if standard hygienization is effective to restore light transmittance. The detergent used for cleaning was common neutral detergent used for cleaning dishes. Transmittance measurements were performed on PET samples after 1 week, 2 weeks and 3 weeks. Confocal microscopy, SEM and EDS were also performed on the samples. SEM was performed with a magnification of 1.39 kX and the potential was 15 kV.

2.3 JxV measurements

JxV measurements: For measurements an HP benchtop was connected to the energy monitoring system. The connection was done for each of the 14 sets and an HP benchtop multimeter used with the ammeter function to measure the forward and reverse current. In this work we report measurements relative to one set of panels that was not under a shadow throughout the 10 months when the measurements took place.

3. Results and Discussion

3.1 Efficiency of the OPV panels

In the period between August/2018 and July/2019 several J xV measurements were done. The panels were connected two by two in series. Every set of 2 panels was then connected in parallel with the others. Measurements in dark and under different conditions of illumination and temperature were also done.

On Figure 3, measurements of the current density (J) versus the voltage (V) are presented. These measurements were done in daylight. Chart 3 is a plot of measurements done on August 31/2018 and November 30/2018 under illumination.

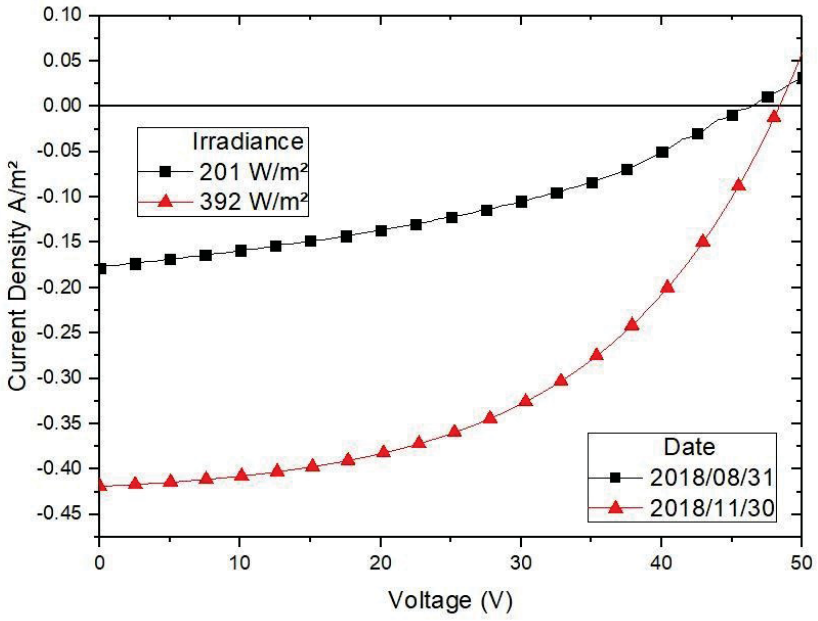

Figure 3: J x V curve. Measurements of one set OPV panels placed on top of the bus shelter made under illumination.

Performance of OPV panels varies according to the climatic conditions. Solar irradiation was 51% higher in November 30/2018 compared to August 31/2018. This difference indicates that a higher efficiency of the panels should be expected from the November measurements due to greater accumulation of solar radiation[1].

To calculate the efficiency of the solar panels we took the measurements done on August 31/2018 and November 30/2018 in one of the sets of panels and used equation (1).

$$\eta = \frac{J_{sc} V_{oc} FF}{P_{in}} \qquad (1)$$

Where η is the efficiency, V_{OC} is the open circuit voltage, J_{SC} is the short circuit current density, FF is the fill factor and P_{in} is the input power density. In table 1 measured quantities and calculated values are presented.

Table 1 Measured and calculated values

Date	V_{oc} (V)	J_{SC} (A/m^2)	FF	P_{in}(W/m^2)	η (%)
2018/08/31	46.34	0.18	0.38	201	3.16
2018/11/30	48.38	0.41	0.51	392	3.27

The efficiency calculated for both dates is around 3% and is considered satisfactory for OPV based panels. It is not possible to affirm to what extent soiling affected influenced the efficiency of the panels in the 3 months period between measurements. In order to better understand the performance of the OPV panels, measurements of $J\ x\ V$ and J_{sc} and V_{oc} will continue in the next few months and will be then compared to measurements from 2018. Measurements in dark will also be made to study degradation of the solar panels.

In table 2 measurements of short circuit current density (J_{SC}) and open circuit voltage (V_{OC}) at different dates for different illuminances are shown. As expected V_{OC} and J_{SC} values increase for higher temperatures and with higher solar irradiance.

Table 2 I_{sc} and V_{oc} measurements

Measurement count	Date	V_{oc} (V)	J_{sc}(A/m^2)	T (^{o}C)	Irradiance (W/m^2)
1	Aug 29/2018	49.48	0.343	15	570.38
2	Sep 12/2018	44.42	0.111	14	110.76
3	Sep 19/2018	50.39	0.423	19	617.00
4	Sep 24/2018	50.44	0.415	20	613.04
5	Oct 22/2018	50.19	0.287	19	231.87
6	May 03/2019	44.91	0.228	18	587.05
7	June 13/2019	38.1	0.072	16	112.73

3.2 Transmittance and Microscopy

Although Curitiba dust levels are not high, light transmittance on PET is affected when samples are exposed to the open environment. After 7 days exposed, samples that were not submitted to any cleaning treatment had a 5% loss in light transmittance while samples cleaned with detergent or samples that received a hydrophobic film (NT70) showed no loss in transmittance. After 2 weeks the loss in transmittance was 7% for samples with no treatment, 3% for samples treated with hydrophobic film and under 1% for samples exposed for 2 weeks and then cleaned with detergent .

The final light transmittance measurements were done on samples exposed to the open environment for 3 weeks. Light transmittance of PET samples that were not cleaned had a 20% loss in the light transmittance while the samples treated with hydrophobic film had a loss of 15% in light transmittance and samples that were cleaned with detergent after exposure had a loss of 4% in light transmittance.

Confocal microscopy on PET samples shows progressive soiling accumulation after 1 week, 2 weeks and 3 weeks of exposure (Figure 5). SEM of the samples after 3weeks (Figure 6) reveals soiling accumulation on a sample exposed without any treatment. In samples treated with hydrophobic film, soiling accumulation was concentrated on punctual spots. Samples exposed and then cleaned prior to SEM showed a clear surface with no soiling spots.

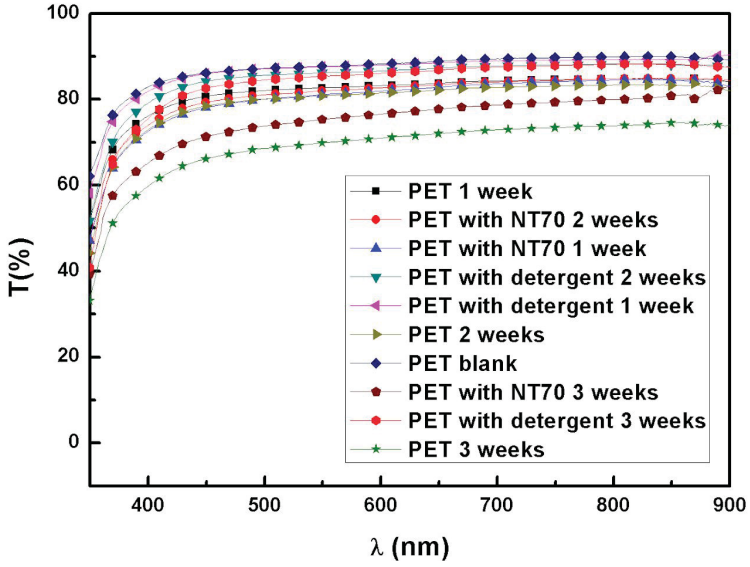

Figure 4: Transmittance measurements on PET samples. The blank is PET with no treatment and no exposure. Treated and untreated samples were exposed on the top of the bus shelter for periods of 1-3 weeks.

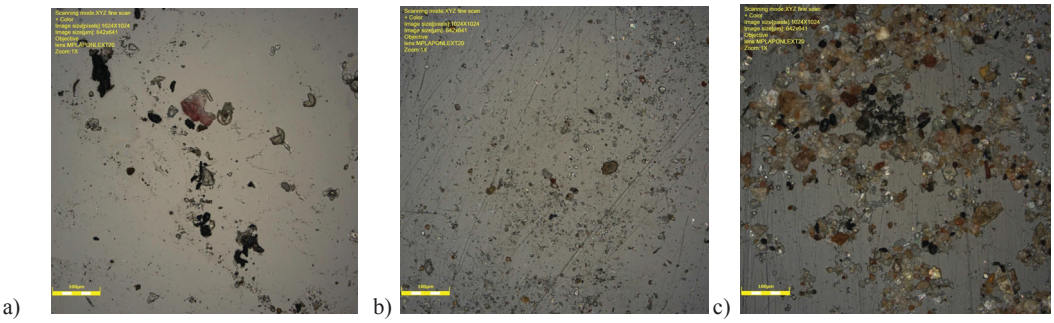

Figure 5: Confocal microscopy of the samples after a) 1 week, b) 2 weeks and c) 3 weeks of exposure.

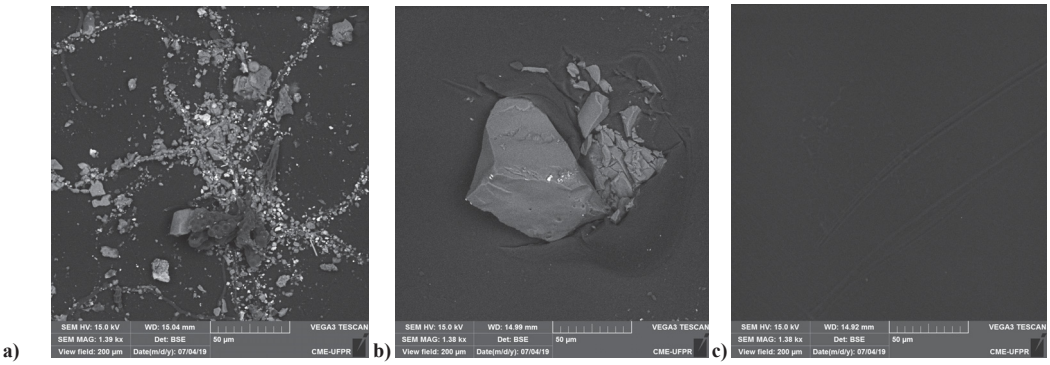

Figure 6: SEM on a view field of 200 µm a) sample with 3 weeks of exposure b) sample cleaned NT70 cleaning, c) sample cleaned with detergent.

4. Conclusions

Soiling affects light transmittance and cleaning with common detergent restores light transmittance. Application of hydrophobic film delays the need for cleaning. Although Curitiba is not in a region with moderate amount of dust (Ghazi, 2014) soiling affects the performance of solar panels.

During the 10 months of this work the setup of the panels and energy monitoring system proved to be reliable. In the next two years we will continue to measure IxV, V_{oc} and I_{SC} to compare the efficiency of the panels with the values measured in the first months of use.

It is important to follow the efficiency of an OPV panels setup under real use conditions. Degradation studies of the panels under real use conditions should be done as they are critical to evaluate the reliability of this kind of system for the use in urban furniture.

5. Acknowledgements

The authors acknowledge Curitiba Prefecture, Urban Planning Secretariat (URBS) for donating the bus shelter, Sunew for manufacturing the solar panels and Jchebly for donating the panels. We thank CNPq for financial support and UFPR Microscopy Center for technical support.

6. References

Canestraro, C.D., Mello, R.M.Q., Micaroni, L., Roman, L. S., Valaski, R. 2007. Organic photovoltaic devices based on polythiophene films electrodeposited on FTO substrates. Solar Energy Materials and Solar Cells. Vol. 91, Issue 8, 684-688.

Cava, C. E., Roman, L. S., Salvatierra, R. V., Zarbin, A. J. G.. 2012. ITO‐Free and Flexible Organic Photovoltaic Device Based on High Transparent and Conductive Polyaniline/Carbon Nanotube Thin Films. Advanced Functional Materials. Vol 23, Issue 12, 1490-1499.

Ghazi, Sanaz, Sayigh, Ali, Ip, Kenneth. 2014. Dust effect on flat surfaces - A review paper. Renewable and Sustainable Energy Reviews. 33, 742-751.

Hengevoss, D., Baumgartner, C., Nisato, G., Hugi, C. 2016. Life Cycle Assessment and eco-efficiency of prospective, flexible, tandem organic photovoltaic module. Solar Energy, Vol. 137, 317-327.

Hosel, M., Krebs, F. C., Soendergaard, R.R. 2012. Roll‐to‐Roll fabrication of large area functional organic materials. J Polym Sci Part B: Polym Phys, Vol 51, 1, 16-34.

Inganas, O. 2018. Organic Photovoltaics over Three Decades. Advanced Materials 30(35):1800388.

Kazmerski, L.L., Qaraghuli, A. A., Sarver, T. 2013. A comprehensive review of the impact of dust on the use of solar energy: History, investigations, results, literature, and mitigation approaches. Renewable and Sustainable Energy Review, 22, 698-733.

Krebs, F.C. et al. Worldwide outdoor round robin study of organic photovoltaic devices and modules. 2014. Solar Energy Materials and Solar Cells. Vol 130, 281-290.

Leitman, J., Rabinovitch, J., 1996. Urban Planning in Curitiba. Scientific American, Vol. 274, Issue 3.

Wouk de Menezes, L., Renzi, W., Marchiori, C., Oliveira, C., Von Kieseritzky, F., Duarte, J. L., Roman, L. (2018). Nonradiative Energy Transfer Between Porphyrin and Copolymer in Films Processed by Organic Solvent and Water-Dispersible Nanoparticles with Photovoltaic Applications. The Journal of Physical Chemistry C. 122. 10.1021/acs.jpcc.8b00390.

Appendix C

Patent

Utilization model submitted to the Brazilian institute of industrial property (INPI)

INSTITUTO NACIONAL DA PROPRIEDADE INDUSTRIAL

18/02/2021 870210015959 11:03

0000421930119469

Manifestação sobre a Opinião Preliminar

Número do Processo: BR 20 2020 011998 8

Dados do Depositante (71)

Depositante 1 de 1

Nome ou Razão Social: UNIVERSIDADE FEDERAL DO PARANA
Tipo de Pessoa: Pessoa Jurídica
CPF/CNPJ: 75095679000149
Nacionalidade: Brasileira
Qualificação Jurídica: Instituição de Ensino e Pesquisa
Endereço: Rua João Negrão, 280 2o andar
Cidade: Curitiba
Estado: PR
CEP: 80010-200
País: Brasil
Telefone: (41) 3360 7441
Fax: (41) 3360 7416
Email: coord.pi@ufpr.br

Referência Petição

Pedido : BR202020011998-8

Documentos anexados

Tipo Anexo	Nome
Esclarecimento	Esclarecimento INPI.pdf
Reivindicações	Reivindicações_com grifos.pdf
Reivindicações	Reivindicações_versão limpa.pdf

Declaração de veracidade

☑ Declaro, sob as penas da lei, que todas as informações acima prestadas são completas e verdadeiras.

PETICIONAMENTO ELETRÔNICO

Esta solicitação foi enviada pelo sistema Peticionamento Eletrônico em 18/02/2021 às 11:03, Petição 870210015959

Appendix D

Urban sustainability project

Project written by request from Curitiba City Hall

PROTÓTIPO DE ESTAÇÕES-TUBO COM MÓDULOS FOTOVOLTAICOS ORGÂNICOS (OPV)

PROFESSORA DR[A] LUCIMARA STOLZ ROMAN
MSC. ANNA GABRIELLA TEMPESTA

RESUMO

O uso de tecnologias solares tem aumentado no mundo todo e faz parte do esforço para conter a crise climática associada à ampla utilização de combustíveis fósseis. Dentre as tecnologias solares, aquelas de menor impacto ambiental são as baseadas em polímeros orgânicos (OPV). Os módulos solares de OPV podem ser impressos sobre substrato flexível, tal como plástico PET, o que os torna especialmente interessantes para utilização sobre superfícies curvas. Em 2016 o laboratório de dispositivos semicondutores nanoestruturados (DiNE) da UFPR propôs à URBS testar a instalação de módulos OPV em uma estação-tubo. A URBS cedeu uma estação-tubo inutilizada para a UFPR e a mesma foi instalada no campus Politécnico. Sob orientação da Professora Lucimara Roman testou-se a eficiência e a resiliência de módulos solares orgânicos de um fabricante. Com base nessa prova de conceito, propõe-se agora fazer a instalação de módulos OPV em 2 estações-tubo que serão colocadas em uso. Cada uma das estações terá painéis de um fabricante diferente. O laboratório DiNE/UFPR ficará responsável por fazer acompanhamento técnico de todo o projeto da instalação ao monitoramento do desempenho dos módulos solares de cada uma das duas estações-tubo. Uma vez que a tecnologia seja validada em reais condições de uso e que se tenha um comparativo do desempenho dos módulos OPV de dos dois fabricantes, a Prefeitura Municipal de Curitiba poderá utilizar o relatório técnico para reproduzir o mesmo projeto em outras estações-tubo.

Appendix E

Work presented in conferences

E.1 List of conference works

1. Dust and Efficiency of Organic Photovoltaics Panels. Fabiana de Brito, A. G. Tempesta, L. C. Mariano, Lucimara S. Roman. Brazil MRS Meeting, 2019

2. Organic Photovoltaic and Urban Sustainability. T. R. C. dos Santos, A. G. Tempesta, K. R. M. Pacheco, L. C. Mariano, L. S. Roman. Brazil MRS Meeting, 2019

3. An application of organic photovoltaic cells (OPV) plant to provide electric power for a bus station tube type. Luiz Carlos Mariano, Anna Gabriella Tempesta, Kaike Rosivan Maia Pacheco, Talitha Ramos Canabarra dos Santos, Lucimara Stolz Roman. Brazil MRS Meeting, 2019

4. Dust and efficiency of organic photovoltaic panels on different surfaces. Fabiana de Brito, Anna Gabriella Tempesta, Talitha Ramos Canabarra dos Santos, Lucimara Stolz Roman. Brazil MRS Meeting, 2021

5. Organic Photovoltaic in an Urban Environment with the author(s) Talitha Ramos Canabarra dos Santos , Anna Gabriella Tempesta , Luiz Carlos Mariano , Kaike Rosivan Maia Pacheco, Lucimara Stolz Roman. Brazil MRS Meeting, 2021

6. "Estação de Pesquisa Tubo de Ensaio": An Application of OPVs. Júlia Ketzer Majewski , Anna Gabriella Tempesta , Talitha Ramos Canabarra dos Santos , Fabiana de Brito , Lucimara Stolz Roman. Brazil MRS Meeting, 2021